Aalto Universtiy
School of Science and Technology
Faculty of Information and Natural Sciences
Degree programme of Communication Engineering

Tomasz Burzanowski

LTE Multicodeword-MIMO: Hybrid-ARQ Perfomance Studies

Master's Thesis
Espoo, December 3, 2010

Supervisor: Professor Olav Tirkkonen, Aalto University
Instructor: Professor Olav Tirkkonen, Aalto University

Aalto University
School of Science and Technology
Faculty of Information and Natural Sciences
Degree Programme of Communication Engineering

ABSTRACT OF
MASTER'S THESIS

Author: Tomasz Burzanowski

Title of thesis:
LTE Multicodeword-MIMO: Hybrid-ARQ Perfomance Studies

Date:	December 3, 2010	**Pages:** 10 + 80
Professorship:	Data Communications Software	**Code:** S-114-2
Supervisor:	Professor Olav Tirkkonen	
Instructor:	Professor Olav Tirkkonen	

Mobile communication is going through major changes since the introduction of first generation mobile phones. Not only phones, but various handheld devices are starting to use the mobile communication network for internet browsing, multimedia or even online gaming. There is a high need for fast mobile connection and therefore new standards and specifications need to be created to satisfy the consumer requirements.

Long Term Evolution (LTE) is the latest candidate for the next mobile communication standard led by Third Generation Partnership Project (3GPP). LTEs main features are high throughput, low latency, simple architecture and low operating costs.

Since mobile data transmission is a non linear process, a simulator is built to model the procedure. Simulator made for this thesis was written in MATLAB meeting the 3GPPs set standards for LTE. Three different Multiple Input Multiple Output (MIMO) downlink HARQ scenarios were created and their performance was evaluated.The main focus of this thesis is the performance comparison of the three downlink scenarios; however the verification of the simulator model plays also a significant role in this work.

Keywords:	LTE, MIMO, HARQ, Throughput, Blanking, Non-blanking, Link adaptation, LTE downlink simulator
Language:	English

Aalto-yliopisto
Teknillinen korkeakoulu
Informaatio- ja luonnontiedeiden tiedekunta
Tietoliikennetekniikan koulutusohjelma

DIPLOMITYÖN
TIIVISTELMÄ

Tekijä: Tomasz Burzanowski

Työn nimi:
LTE Multicodeword-MIMO: Hybrid-ARQ Perfomance Studies

Päiväys:	3. joulukuuta 2010	**Sivumäärä:** 10 + 80
Professuuri:	Tietoliikennetekniikka	**Koodi:** S-114-2
Työn valvoja:	Professori Olav Tirkkonen	
Työn ohjaaja:	Professori Olav Tirkkonen	

Langattomassa tiedonsiirrossa on tällä hetkellä meneillään suuria muutoksia, sitten ensimmäisen matkapuhelinsukupolven käyttöönoton. Uusia datapuhelimia, kuten myös kämmentietokoneita käytetään internetin selaamiseen, videoiden katselemiseen ja pelaamiseen matkapuhelinverkon kautta. Voidaakseen tyydyttämään kuluttajien vaatimukset, tarve uusien langattoman tiedonsiirron normien luomiseen on merkittävä.

Long Term Evolution (LTE) on, Third Generation Partership Project:in (3GPP) johtama, ehdokas seuraavaksi matkapuhelinsukupolven standardiksi. LTE:n ominaisuuksiin kuuluvat mm. korkea suoritusteho, matala latenssi, yksinkertaisuus ja alhaiset kustannukset. Tulevassa standardissa on aihealueita, joita ei ole varsinaisesti tutkittu akateemisessa maailmassa kuten Hybrid Automatic Repeat Request:in (HARQ) suorituskykyä.

Koska langaton tiedonsiirto on epälineaarinen prosessi, sitä mallinnetaan simulaattorin avulla. Simulaattori on tehty MATLAB ympäristössä LTE:n standardien mukaisesti. Kolme eri Multiple Input Multiple Output (MIMO) downlink HARQ skenaariota luotiin ja niiden suorituskykyä arvioitiin. Pääpaino työn tutkimukselle kohdistuu kolmen HARQ:n suorituskykyyn, tosin simulaattorimallin todistaminen on myös keskeinen osa tätä työtä.

Avainsanat: LTE, MIMO, HARQ, suorituskyky, Blanking, Non-blanking, linkki adaptaatio, LTE simulaattori
Kieli: englanti

Acknowledgements

I would like to express my sincere gratitude to my supervisor Prof. Olav Tirkkonen and MSc. Kalle Ruttik for their support and guidance and patience during the course of this work. Their encouragement and support has always been a source of motivation for me to explore various aspects of the topic. Discussions with them have always been instructive and insightful and helped me to identify my ideas.

Finally, I am very grateful to my parents Halina and Aleksy and my younger brother Adam Burzanowski for their sacrifices, unremitting motivation, love and their continuous support during my stay at Aalto University School of Science and Technology in Otaniemi.

Espoo December 3, 2010

Tomasz Burzanowski

Abbreviations and Acronyms

3G	3rd Generation
3GPP	3rd Generation Partnership Project
ACK	Postive Acknowledgement
AMC	Adaptive Modulation and Coding
ARQ	Automatic Repeat Request
AWGN	Additive White Gaussian Noise
BER	Bit Error Rate
BLER	Block Error Rate
BPSK	Binary Phase Shift Keying
CDD	Cyclic Delay Diversity
CIR	Channel Impulse Response
CP	Cyclic Prefix
CQI	Channel Quality Indicator
CRC	Cyclic Redundancy Check
dB	Decibel
DFT	Discrete Fourier Transform
DRX	Discontinuous Reception
DVB	Digital Video Broadcasting
DwPTS	Downlink Pilot Timeslot
E-UTRAN	Evolved-UMTS Terrestial Radio Access Network
eNodeB	Evolved Node Base Station
FDD	Frequency Division Multiplexing
FEC	Forward Error Correction
FFT	Fast Fourier Transform
GB	Giga Byte
GHz	Giga Hertz
GP	Guard Period
GUI	Graphical User Interface
HARQ	Hybrid Automatic Repeat Request
Hz	Hertz
ICI	Intercarrier interference
IDFT	Inverse Discrete Fourier Transform

IFFT	Inverse Fast Fourirer Transform
ITU	International Telecommunication Union
ISI	Intersymbolic interference
LMS	Least Minimum Square
LS	Least Square
LTE	Long Term Evolution
MAC	Medium Access Control
MCS	Modulation and Coding Scheme
MIMO	Multiple Input Multiple Output
MMSE	Minimum Mean Square
NACK	Negatice Acknowledgement
NDI	New Data Indicator
OFDM	Orthogonal Frequency Division Multiplexing
PAPR	Peak-to-Average Power Ratio
PCCC	Parallel Concatenated Convolutional Code
PDCP	Packet Data Convergence Protocol
PDU	Protocol Data Unit
QAM	Quadrature Amplitude modulation
QoS	Quality of Service
QPSK	Quadrature Phase Shift Keying
RAN	Radio Access Network
RB	Resource Block
RE	Resource Element
RLC	Radio Link Control
RTT	Round Trip Time
RV	Redundancy Version
SAP	Service Access Point
SB	Subblock
SDU	Service Data Unit
TDD	Time Division Multiplexing
TKK	Teknillinen Korkeakoulu
TTI	Transmission Time Intervall
UE	User Equipment
UMTS	Universal Mobile Telecommunication System
UpPTS	Uplink Pilot Timeslot
VLSI	Very-large-scale integration
WCDMA	Wideband Code Divison Multiple Access
WiMax	Worldwide Interoperability for Microwave Access

Contents

1 Introduction **1**

1.1 Background 1

1.2 Motivation and problem statement 2

1.3 Outline 3

2 OFDM Principle **4**

2.1 Multicarrier-modulation 4

2.2 Orthogonal frequency division multiplexing 6

2.3 Model 11

3 Background **13**

3.1 LTE standardization 13

3.2 LTE key features and requirements 15

3.3 LTE frame structure 16

3.3.1 Type 1 (FDD) and Type 2 (TDD) 17

3.3.2 Slot structure 18

3.3.3 Cyclic prefix 20

3.4 Modulation 20

3.4.1 QPSK, 16-QAM and 64-QAM 21

3.4.2 Pilot structure 25

3.4.3 Channel estimation 26

3.5 Link adaptation 27

3.5.1 Adaptive Modulation and Coding 28

3.6 MIMO 29
3.6.1 Basics 30
3.6.2 Spatial multiplexing 30
3.6.3 Pre-coding 31
3.6.4 Transmit diversity 33
3.7 Multicodeword-MIMO HARQ 34
3.7.1 ARQ protocol categories 34
3.7.2 Chase Combining and Incremental Redundancy 38
3.7.3 Multicodeword-MIMO HARQ alternatives 39
3.7.3.1 Independent 40
3.7.3.2 Blanking 40
3.7.3.3 Non-blanking 40

4 LTE Downlink **42**
4.1 RLC Layer 42
4.2 MAC Layer 44
4.2.1 Multiplexing and mapping 44
4.2.2 Scheduling 45
4.2.3 Discontinuous Reception (DRX) 47
4.2.4 HARQ 47
4.3 PHY Layer 47
4.3.1 Channel coding 48
4.3.1.1 CRC 48
4.3.1.2 Turbo coding 49
4.3.2 Modulation 50
4.3.3 HARQ 51

5 Simulator **53**
5.1 System model 53
5.1.1 Transmitter 55
5.1.2 Channel 55

5.1.2.1 Winner II model 56
5.1.2.2 Typical Urban model 56
5.1.3 Receiver 57
5.1.4 Simulator verification 58
5.1.4.1 BER QPSK 59
5.1.4.2 BER 16-QAM 59
5.1.4.3 BER 64-QAM 60
5.1.4.4 HARQ functionality 62
5.1.4.5 Transmit diversity 66
5.1.4.6 Link adaptation 67
5.1.4.7 MIMO transmission 67

6 Multicodeword-MIMO Performance **71**
6.1 Simulation Results 71
6.2 Comparison 73

7 Conclusion **75**
7.1 Future work 76

References **77**

Chapter 1

Introduction

As introduction some background information with estimation of upcoming trends in mobile communications is given. Next motivation and problem statement for writing this thesis are described, followed by an outline of the remaining document.

1.1 Background

Due the increasing demand for higher data rates for wireless communication systems and the growth of mobile data transfer usage, the wireless communication area has gained significant attraction for mobile researches and industries worldwide. Mobile broadband is becoming reality and according to [23] out of the estimated 1.8 billion people, who will have broadband by 2012, some two third will be mobile broadband customers and the majority will be served by HSPA (High Speed Packet Access) and LTE (Long Term Evolution).

The third Generation Partnership Project (3GPP) organization has started an international collaboration project to improve the Universal Mobile Telecommunication System (UMTS) and this also can be considered as a milestone towards fourth generation (4G) standardization. The main focus of this project is to establish a mobile broadband that will support the future demand of mobile users like efficiency improvement, service enhancement, lower maintenance and usage costs and better integration with other standards. Table 1.1 describes the 3GPP group technical specifications [8].

High wireless communication quality and increasing data rates are limited through bandwidth resources. Therefore rapidly growing number of users sharing the same resource, more advanced technologies are needed to achieve satisfying spectral ef-

Release	Specification	Date
Release 99	UMTS 3G networks, CDMA air interface	March 2000
Release 4	All-IP Core Network	March 2001
Release 5	IMS and HSDPA	March - June 2002
Release 6	WLAN, HSUPA and MBMS	Dec. 2004 - March 2005
Release 7	HSPA+ and EDGE Evolution.	Dec. 2007
Release 8	LTE	December 2008
Release 9	WiMax and LTE/UMTS Interoperability	Dec. 2009
Release 10	LTE Advanced	March 2011?

Table 1.1: Technical specification published by 3GPP

ficiency. Technologies like Orthogonal Frequency Division Multiplexing (OFDM) and multiple input, multiple output (MIMO), can improve the performance of current wireless communication systems. For future mobile communications system LTE is the next step and basis for future enhancements. LTE is the first cellular communication system optimized to support packet-switched data services, where packetized voice communication is just one part of it.

1.2 Motivation and problem statement

Since sending mobile data over certain channel is a highly non linear process, there is a need building a tool in form of a simulator to gain access to different subjects related with mobile communication as bit error rates (BER), channel estimation and throughput calculations.

The main focus of this thesis is to build a LTE downlink simulator using an older generation simulator as a reference and to explore different HARQ implementation methods, which were discussed in [3] in 2006, but which are very little examined in the academic world. In 2010, for LTE-Advanced the discussion reconsidering HARQ process bundling for multicodeword-MIMO to boost the spectral efficiency and trying to keep the feedback overhead low [25]. The simulator has been developed by TKK Communication Engineering Department in MATLAB coding environment and a long term goal is to have a clean structured tool for demoing purposes at the Helsinki University of Technology. By structured is meant, that different functions from different layers e.g. Physical (PHY) layer or Medium Access Control (MAC) layer are separated according to the standards set by 3GPP.

This thesis investigates some of LTEs downlink physical layer algorithms, their performance and comparison in data throughput. Hybrid Automatic Repeat reQuest (HARQ) is described in the Chapter 3.7. There are three different simulation cases where the throughput is calculated for each case and each signal-to-interference-noise ratio (SINR). The following HARQ process scenarios are investigated in this paper:

- Two codewords and two independent HARQ processes
- Two codewords and one independent HARQ process
  - Blanking
  - Non-blanking

Where the second case is divided into two sub cases, blanking and non-blanking. Detailed description of the simulation scenarios is found in Chapter 3.7.

1.3 Outline

Chapter 2 describes the principle of OFDM transmission used in LTE standard, including multicarrier modulation and frequency division multiplexing. At the end of this chapter a mathematical model of an OFDM transceiver is shown and explained.

In Chapter 3, the LTE standard is described beginning with a general standardization process followed by key features of LTE. Furthermore more detailed view of LTE is given by introducing different frame structures, modulation, link adaptation and multi antenna transmission as well as three different HARQ procedures.

Chapter 4 is devoted to more detailed view of LTE downlink transmission, where the functionalities of the different layers are introduced and explained.

In Chapter 5 the model used in the simulator built for this thesis is described in details, including the verification tests to prove it working in correct way.

In Chapter 6 three different HARQ methods are investigated including simulation parameters and received graphical results.

In last Chapter 7 the conclusions from the simulation are listed and future work topics are suggested.

Chapter 2

OFDM Principle

This chapter describes the principle of Orthogonal Frequency Division Multiplexing (OFDM). In the first section, a general introduction to multicarrier modulation including mathematic descriptions and illustrations is given.

Next. a more detailed view of OFDM including basic characteristics and relation between time and frequency domain is given. Also concept of cyclic prefix with OFDM is introduced and how it is to be implemented in the LTE standard.

Finally a mathematic model of an OFDM transceiver including transmitter, receiver and a simple one tap equalizer is illustrated.

2.1 Multicarrier-modulation

Multicarrier-modulation was first introduced in the 50's, but completed in the 60's and forms the basis of the OFDM modulation principle. In this technique, the available bandwidth W is divided into number of N_c sub bands or sub carriers, where each of them has the width of $\Delta f = \frac{W}{N_c}$. This is illustrated in Figure 2.1.

Instead of transmitting the data symbols serially, the multi-carrier transmitter divides the symbols into blocks of N_c data symbols which are transmitted in parallel by modulating each sub carrier. Therefore the symbol duration for a modulated carrier is $T_u = \frac{1}{W}$ [21].

The multi-carrier signal can be described as a set of modulated carriers [22]:

$$s(t) = \sum_{k=0}^{N_c-1} x_k \Psi_k(t) \tag{2.1}$$

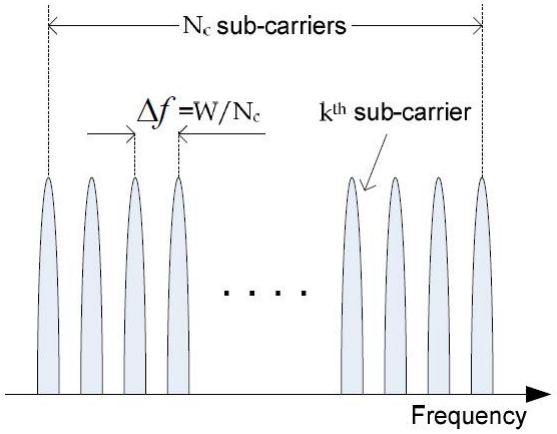

Figure 2.1: Division of bandwidth into N_c sub carriers

where

x_k is the data symbol modulating the k^{th} sub-carrier

$\Psi_k(t)$ is the modulation waveform at the k^{th} sub-carrier

$s(t)$ is the multi-carrier modulated signal

Figure 2.2 illustrates the process of generating a multi-carrier modulated signal. To tone down the effects of fading when designing a multi-carrier system the following steps can be taken into account [15].

- The data symbol duration can be made longer than the maximum excess delay of the channel in time domain $T_u >> \tau_{max}$.
- The bandwidth of the sub carriers can be made small compared to the coherence bandwidth of the channel in frequency domain $B_{coh} = \frac{W}{N_c}$. The sub bands now experience flat fading so the equalization can be reduced to a single complex multiplication per carrier.

It is to be noted, that these steps are adressing the same subject viewed from different angle. The first looks at the problem from time domain point of view and the second step can be taking into account in the frequency domain.

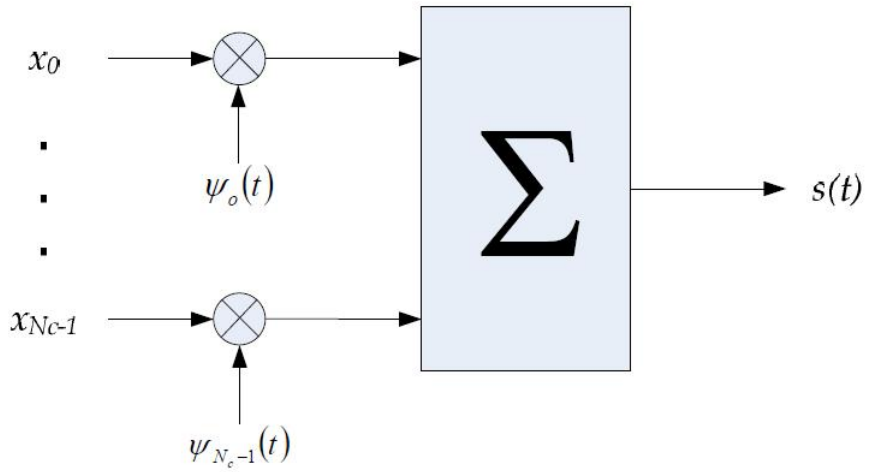

Figure 2.2: Principle of multi-carrier modulation

2.2 Orthogonal frequency division multiplexing

OFDM is a digital modulation method where the signal is divided into several narrow band channels at different frequencies where modulation and multiplexing are combined. The technique was used in the 60's in several high frequency military systems for parallel data transmission. OFDM become more popular when in 1966, Chang [49] patented the structure of it and published a concept of using orthogonal overlapping multi tone signals for data communication. In 1971, Weinstein and Ebert [29] first introduced Discrete Fourier Transform (DFT) to parallel data transmission system which become part of the modulation and demodulation process. In the 90's OFDM, gained popularity in wide band data communications and today's improvements in very-large-scale integration (VLSI) technology allows fast and cost effective Fast Fourier Transform (FFT) implementation of OFDM systems. It is used as a downlink transmission scheme for LTE and it also used for other radio technologies like WiMax and and Digital Video Broadcasting (DVB).

OFDM transmission can be seen as a kind of multi-carrier transmission, nevertheless some of its basics characteristics which differ from basic multi-carrier of a more narrowband transmission are [21]:

- The use of large number of narrowband subcarriers comparing e.g. to LTE's predecessor Wideband Code Division Multiple Access (WCDMA) where 20 MHz bandwidth would be divided into four 5 MHz subcarriers. In comparison, in OFDM transmission there can be several hundred subcarriers

carrying the data to the same receiver.

- Simple rectangular pulse shaping which corresponds to sinc-square shaped per subcarrier spectrum as illustrated in Figure 2.3
- Tight frequency domain subcarrier packing with subcarrier spacing $\Delta f = \frac{1}{T_u}$, where T_u is per subcarrier modulation symbol time as seen in Figure 2.4

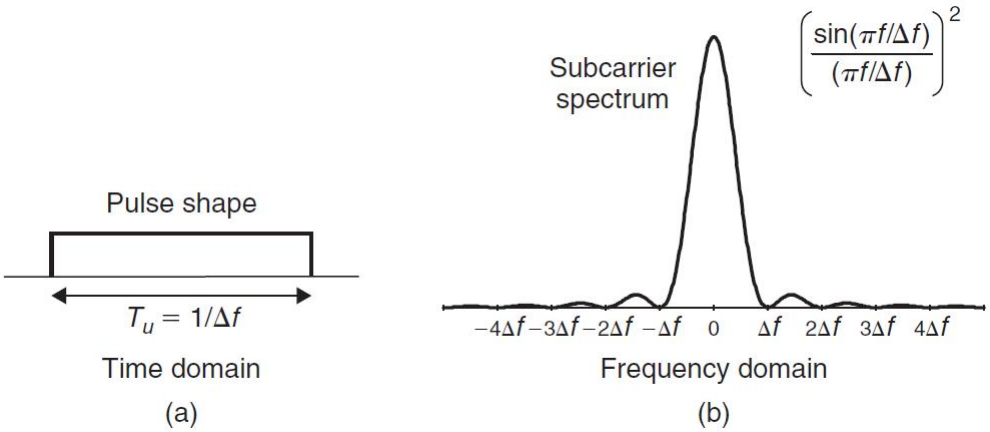

Figure 2.3: (a) subcarrier pulse shape in time and (b) spectrum in frequncy domain

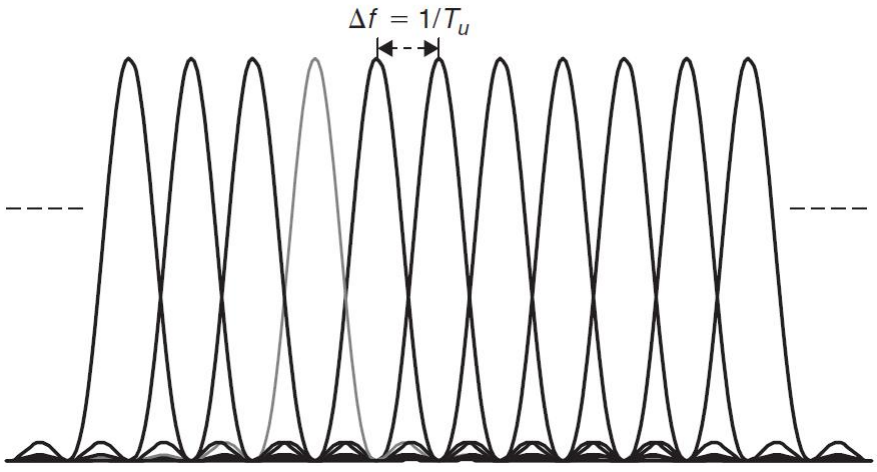

Figure 2.4: OFDM subcarrier spacing

The subcarrier pulses are chosen to be rectangular hence the task of pulse forming and modulation can be performed as a simple mathematical calculation like Inverse Discrete Fourier Transform (IDFT), which is simple and fast to implement as a Inverse Fast Fourier Transform (IFFT). The receiver just needs to perform reverse transform called Fast Fourier Transform (FFT).

The OFDM spectrum is overlapping; nevertheless it is not causing interference due the orthogonal characteristic of the subcarriers. At the subcarrier frequency where the received signal is evaluated all others subcarriers are zero as seen in Figure 2.4.

An OFDM modulator can be mathematically described with help of equation (2.2) [1] and illustrated as shown in Figure 2.5 [21].

$$x(t) = \sum_{k=0}^{N_c-1} x_k(t) = \sum_{k=0}^{N_c-1} a_k^{(m)} e^{j2\pi k\Delta f t} \tag{2.2}$$

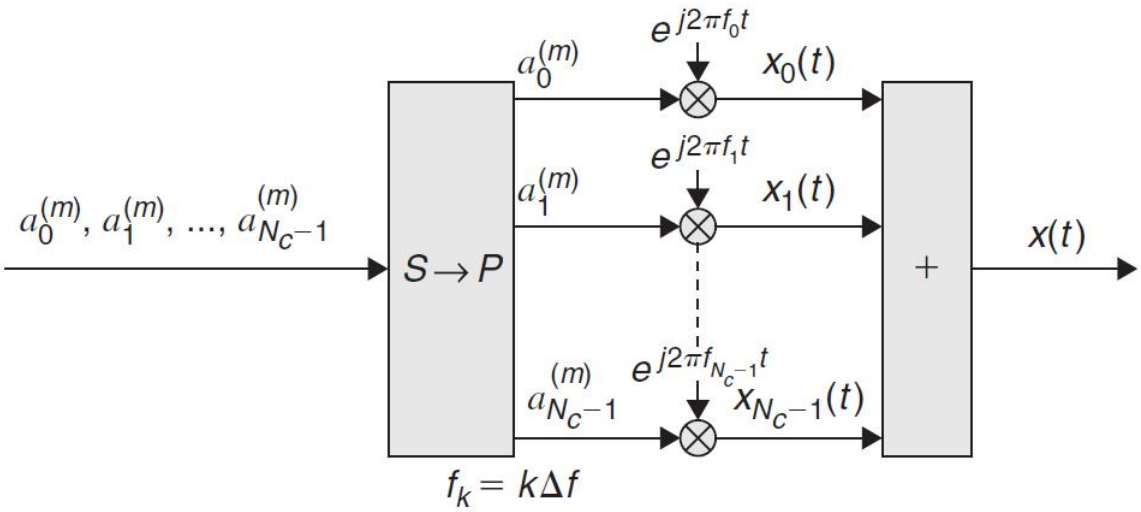

Figure 2.5: OFDM modulation

Where $x_k(t)$ is the k^{th} modulated subcarrier with the frequency $f_k = k\Delta f$ and a_k^m is the modulation symbol applied to the k^{th} subcarrier during the m^{th} OFDM symbol. The modulation symbols can be from any modulation alphabet e.g. QPSK, 16-QAM or 64-QAM.

[1] Valid for time interval $mT_u \leq t < (m+1)T_u$

Physical resource in OFDM transmission can be illustrated as a time-frequency grid as shown in Figure 2.6 [21], where each row is one OFDM subcarrier and each column corresponds to one OFDM symbol.

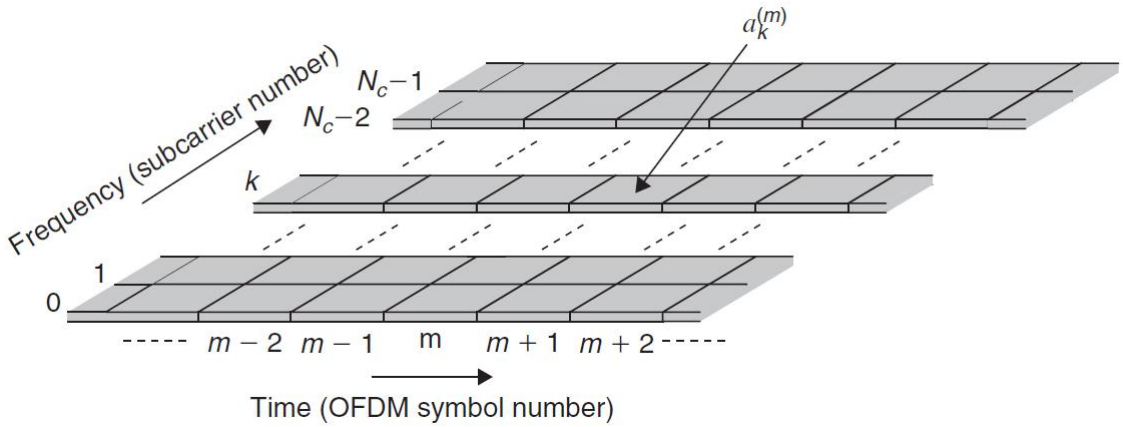

Figure 2.6: OFDM time-frequency grid

As shown in [33], under assumption of perfect time and frequency synchronization and also if the channel does not cause any dispersion in time nor frequency domain and the only degradation source is noise, the transmitted data can be perfectly demodulated. This is because of the orthogonality of the OFDM symbols of the symbol interval T_s:

$$\frac{1}{T_s}\int_0^{T_s} e^{-j2\pi\Delta f(k-m)t}\,dt = \begin{cases} 1 & k=m \\ 0 & k\neq m \end{cases} \tag{2.3}$$

In practice the orthogonality is lost through a frequency selective channel resulting, intersymbolic interference (ISI) and intercarrier interference (ICI) in an OFDM system. In order to minimize these effects the concept of cyclic prefix (CP) was introduced in 1980 [43]. CP is a copy of a tail of the OFDM symbol that is added in front of the symbol as seen in Figure 2.7 from [15]. This so called guard interval is removed at the receiver before demodulation.

The CP length does not necessarily need to cover the whole channel time dispersion therefore there is a tradeoff between power loss and the signal corruption caused by ISI and ICI. At certain point, further reduction of signal corruption due the increase of CP length cannot compensate the additional power loss [2].

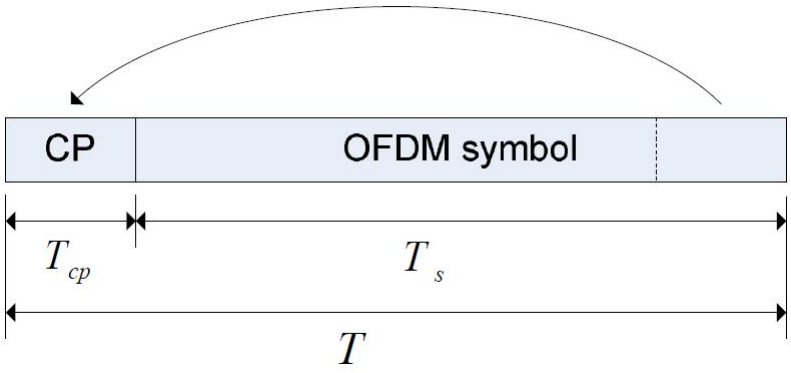

Figure 2.7: Cyclic prefix

As already mentioned, the advantages of CP do not come for free. Due to the guard interval some parts of the signal are not available for data transmission so the energy required transmitting the signal increases with the length of CP and the OFDM symbol rate is also reduced. This loss can be calculated according to [22] in equation (2.4).

$$SNR_{loss} = -10 \log_{10} \left(1 - \frac{T_{cp}}{T} \right) \tag{2.4}$$

where

T_{cp} is the the length of CP

T_s is the symbol time

$T = T_{cp} + T_s$ is the length of transmitted symbol

The parallel transmission of OFDM systems brings many advantages over single carrier systems. The OFDM symbol time is longer than the symbol time of a serial system hence OFDM is less sensitive to multipath and reduces the complexity of the receivers. It is also robust against frequency selective fading since it will affect only a small percentage of the subcarriers, which can be recovered with a proper channel coding. It gives access to frequency domain where each subcarrier can be independently scheduled and adapted to the radio channel conditions to give users the modulation and coding rate depending on the environment. OFDM's

provision of flat sub channels is precious to systems using multiple input and multiple output (MIMO), which are be discussed in section 3.6.

On the other hand OFDM has several drawbacks. Firstly, phase noise causes ISI and other frequency errors can cause ICI. OFDM is also sensitive to the Doppler shift. The amplitude of an OFDM signal has a Gaussian like distribution which means high Peak-to-Average Power Ratio (PAPR). This must be compensated with complex high precision and more expensive analog digital and digital analog converters (ADC, DAC), which need to operate over a wide range. On the receivers side good synchronization is required for the FFT demodulation, hence pilot sequences are used [45]. Pilot tone structure is disucessed in detail in Chapter 3.4.2.

2.3 Model

As described in Section 2.2 an OFDM system can be constructed using IFFT, FFT and CP operations. Figure 2.8 illustrates a discrete OFDM system model [21].

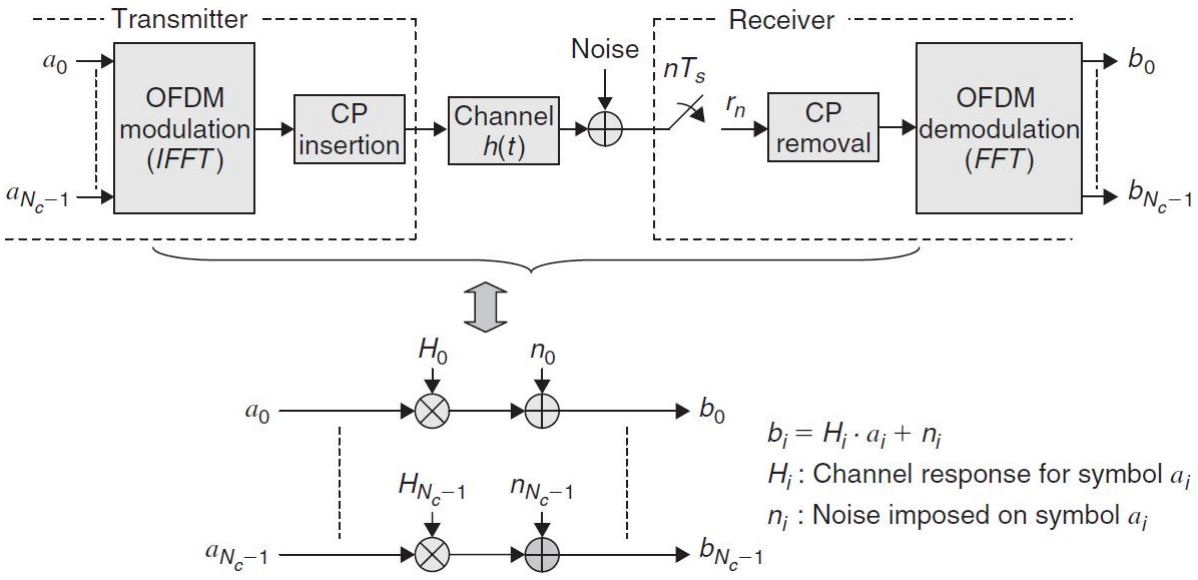

Figure 2.8: Discrete frequency domain OFDM model

OFDM modulation (IFFT), time dispersive radio channel and OFDM demodulation (FFT) can be described as a frequency domain model, where the channel taps H, are resulting from the channel impulse response.

The transmitted symbol a_i is multiplied, which means scaling and phase rotation, by a complex frequency domain channel tap H_i and Additional White Gaussian Noise (AWGN) is added, resulting in the demodulator output symbol b_i. For further processing e.g. data demodulation or channel decoding, the output symbol b_i is multiplied by with the complex conjugate channel tap H_k^* as seen in Figure 2.9. This model is expressed as a one tap equalizer [21].

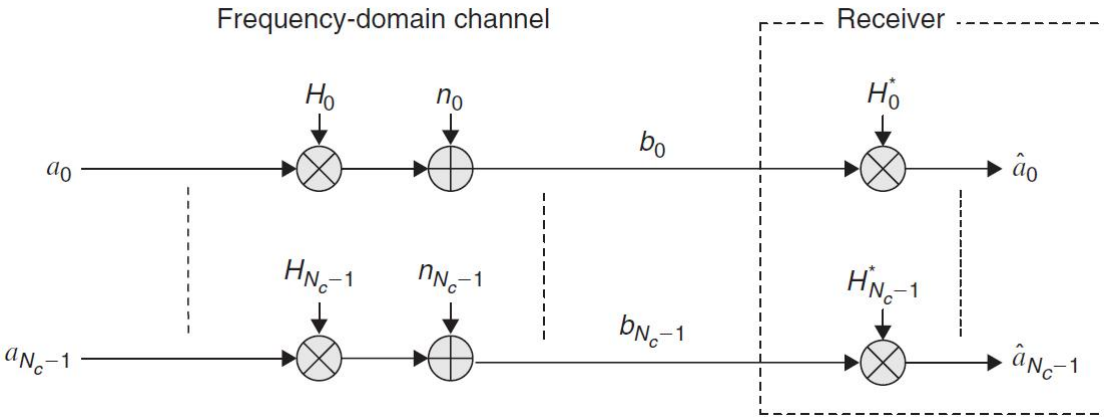

Figure 2.9: Frequency domain OFDM model with one tap equalizer

Chapter 3

Background

In this chapter overall overview of LTE standard is given. Firstly general standardization process and its four phases are described in detail followed by the goals set for the upcoming LTE standard.

Next, LTE's key features and requirements are reviewed and discussed briefly, giving and overview of the standard. Moving on to more detailed description about the layout of two different frame structures where slot structure and cyclic prefix insertion are explained.

Then different digital modulation schemes used in LTE are introduced, illustrated and compared with each other. Pilot tones used as reference signals for channel estimation as well as few channel estimation methods are described.

Furthermore multiple input multiple output (MIMO) basics are briefly summed up, enabling a new dimension in addition to time and frequency, a technique called spatial multiplexing. Also pre-coding and transmit diversity are discussed together with MIMO technique.

Lastly hybrid ARQ and its different implementation methods are illustrated. Moreover three different HARQ scenarios investigated in this Master thesis are reviewed and illustrated with examples.

3.1 LTE standardization

Creating a standard for mobile communication does not happen over one night. Since it is an ongoing process and constantly developed, it can take one to two years until the standard is completed and even longer when products using this standard are commercialized and brought to market. When building standards

from the scratch the time is even longer since there are no components to rely on. Standardization process typically includes four phases which are shown in Figure 3.1 taken from [21].

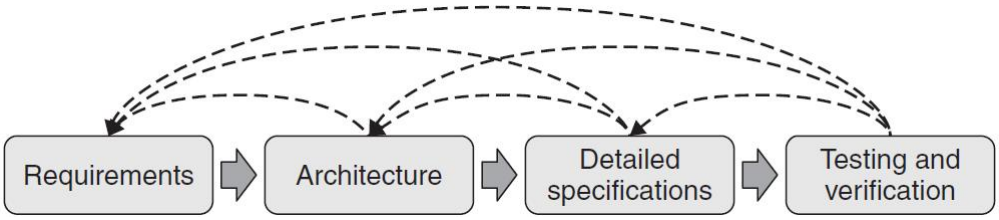

Figure 3.1: Four standardization phases

These phases include:

- *Requirements*, where it is decided what needs to be realized and where the goal is set
- *Architechure*, where the main building blocks and interfaces are fixed
- *Detailed specifications*, where every block and interface are described in detail
- *Testing and verification*, where the specifications are to work in praxis.

Theses phases are of course overlapping and interactive, hence requirements or techniques can be added, dropped or changed during the whole process, depending on the final technical solution.

Standardization process begins with the *requirement phase*, where the basis is decided what must be achieved. This phase is rather short, however well defined requirements can shorten the upcoming phases.

Followed by *architecture phase*, where the building blocks are defined for the construction of the upcoming standard e.g. how to achieve the set requirements. This phase contains decisions about reference points needed to be standardized. Normally this can take some time, since the requirements may change and it might be necessary to take one step back to the previous phase.

After defining the blocks and the interfaces the *detailed specification phase* occurs. The blocks are now described in detail and again it might require going back and forth through the previous states.

At last the specifications must be tested and verified where the final proof for the upcoming standard is set. Naturally during the testing phase some errors

and problems may come up and may again require changes in the specifications. *Testing and verification phase* ends when equipment can be built fulfilling the set requirements and is ready to be set free for the market.

The following goals were set by 3GPP for LTE standard [23]:

- Reduced cost per bit
- Increased service provisioning, meaning more services at lower cost with better user experience
- Flexible use of existing and new frequency bands
- Simplified architecture and open interfaces
- Reasonable terminal power consumption

3.2 LTE key features and requirements

The key features of LTE are described below according to [21], [33] and [45].

The goal is to provide a high data rate, low latency and a packet optimized radio technology which supports flexible bandwidth deployment. The targets for downlink peak data rate requirements are 100 Mbit/s and 50 Mbit/s for uplink, when 20 MHz spectrum is allocated. Both frequency division duplexing (FDD) and time division duplexing (TDD) are supported.

The latency requirements are split over control plane and user plane requirements where round trip time is reduced to 10 ms or less, which provides interactive real time services. Control plane requirements is the time which is needed for user equipment (UE) to switch from non active state to an active one to be able to send or receive data. Side requirement for control plane is number of supported UEs, which is listed to be at least 200 terminals in active state when operating at 5 MHz. Second requirement addresses the time needed to transmit a small IP packet from UE to the radio access network (RAN). LTE provides two to four times better spectral efficiency than Release 6 HSPA, which gives the opportunity to operators to increase number of customers in given spectrum.

LTE system mobility requirements are optimized for low terminal speed, 0-15 km/h, nevertheless mobile terminal speeds up to 350 km/h where slight degradation of performance is allowed. For cell sizes up to 5 km LTE can provide optimum performance meeting spectrum efficiency and mobility requirements, although it can deliver efficient performance for cell size up to 30 km and it can

support maximum cell size up to 100 km, hence no performance requirements are listed for that case.

LTE is also able to coexist and interwork with other 3GPP radio access technologies such as GSM and HSPA. The service handover must be smooth and seamless for users even though UE is in area not covered by the LTE technology.

One of the main features of LTE is the change to a flat all-IP based core network with simplified architecture, which goal is to minimize redundant options and the amount of test cases. In cost and service related aspects operational and maintenance cost are reduced, furthermore low complexity and low power consumption of the mobile terminal is addressed.

Table 3.1 summarizes the key features of LTE system.

Bandwidth	1.25-20 MHz
Duplexing	FDD and TDD
Mobilty	up to 350 km/h
Peak data rate in 20 Mhz	100 Mbit/s downlink, 50 Mbit/s uplink
Modulation	QPSK, 16-QAM and 64-QAM
Channel coding	Turbo code

Table 3.1: LTE system key features and requirements

3.3 LTE frame structure

Figure 3.2 shows the LTE generic frame structure. Each radio frame has the length of 10 ms which contains ten equal sub frames of 1 ms length. The basic time unit is specified as $T_s = \frac{1}{30720000}s$, hence the time of frame length can be specified as $T_{frame} = 307200T_s$ and sub frame as $T_{subframe} = 30720T_s$.

As already stated, LTE can operate in both FDD and TDD. Basically the frames are equal in the structure, furthermore TDD has a special sub frame inserted as seen in Figure 3.4. This special frame is used for the required guard time to switch from uplink to downlink transmission and vice versa. The difference between the frame times type 1 for FDD and type 2 for TDD are discussed in the next section.

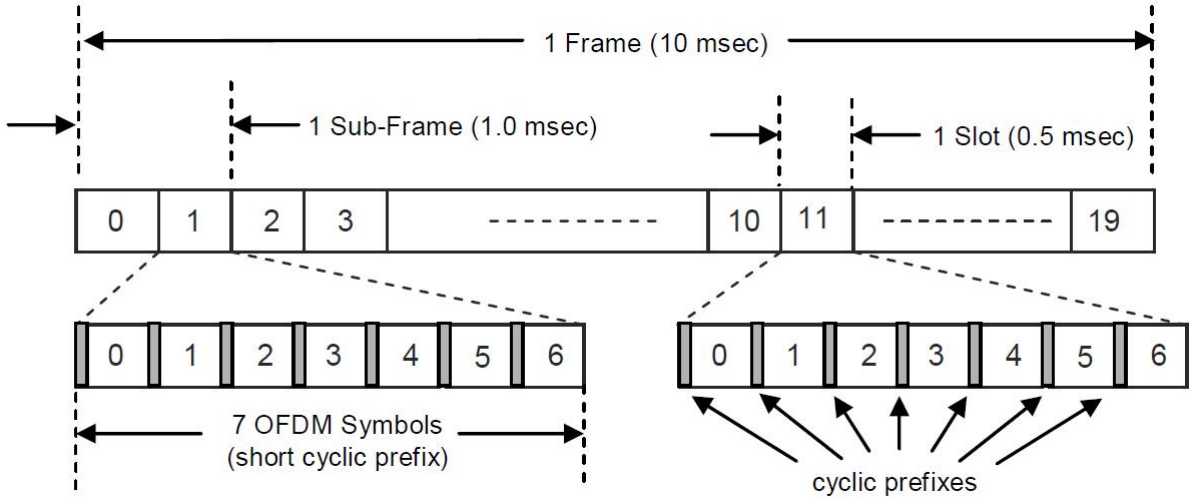

Figure 3.2: LTE generic frame structure

3.3.1 Type 1 (FDD) and Type 2 (TDD)

LTE type 1 frame is designed for FDD and can be used for both half and full duplex FDD transmission modes. The frame has duration of 10 ms and has 20 identical sized slot of 0.5 ms ($T_{slot} = 15360T_s$) length. One sub frame includes two slots, consequently one FDD radio frame has ten sub frames as seen in Figure 3.3 [36]. One half of the frames is used for downlink and the other half is used for uplink transmission, where they are separated in the frequency domain [6].

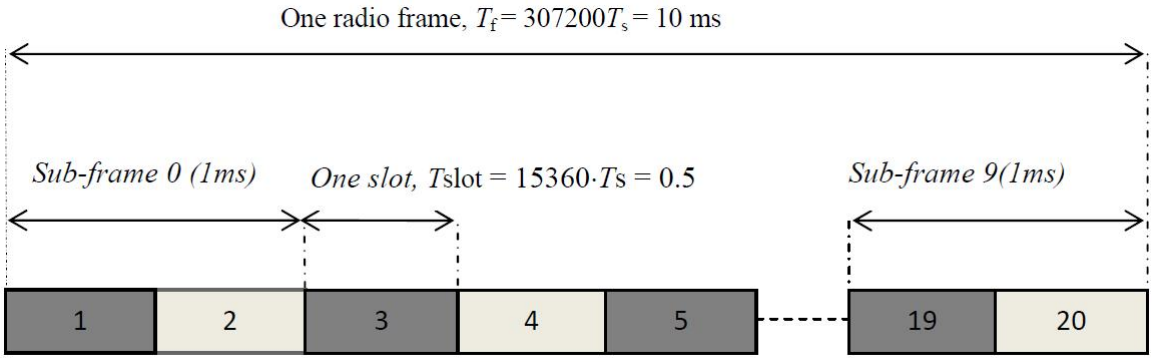

Figure 3.3: LTE type 1 frame structure for FDD

In TDD mode type 2 frame is used, where it consists two same sized half frames with duration of 5 ms. Each of these is separated into five sub frames having

the length of 1 ms as illustrated in Figure 3.4. Again two slots of 0.5 ms length build one sub frame. The earlier mentioned special sub frame is constructed by three fields named Downlink Pilot Timeslot (DwPTS), Guard Period (GP) and Uplink Pilot Timeslot (UpPTS). Three downlink-uplink configurations for 10 ms downlink to uplink switch point periodicity and four 5 ms are specified in [7] as listed in the Table 3.2.

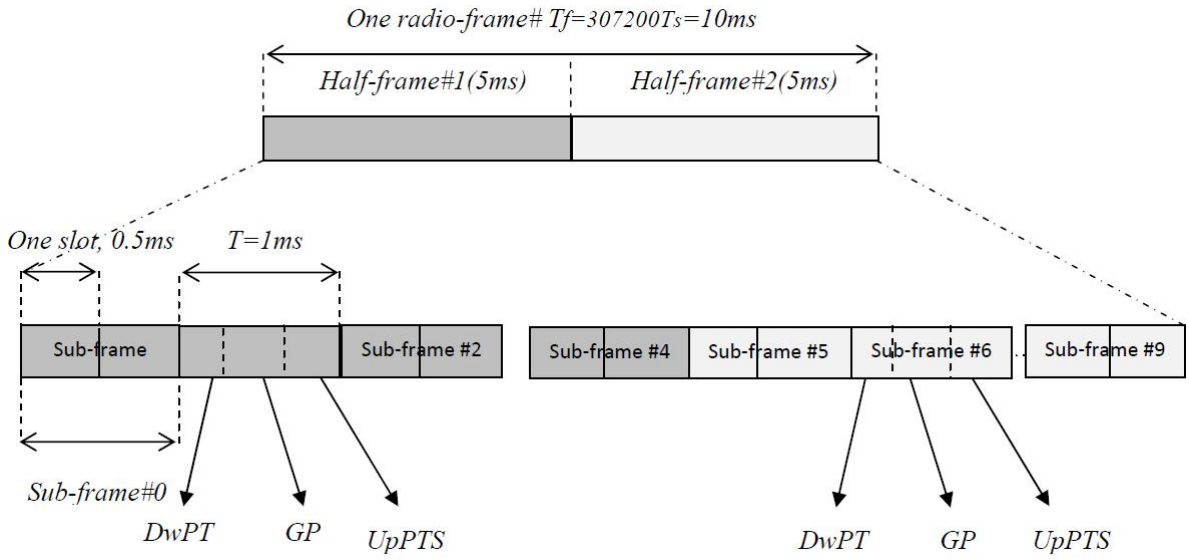

Figure 3.4: LTE type 2 frame structure for TDD

In 5 ms downlink to uplink switch point periodicity special sub frames are used in both half frames, nevertheless for 10 ms special frame is only used in the first half frame. In downlink transmission sub frame 0, 5 and DwPTS are always reserved. In uplink communication UpPTS and the sub frame next to special frame are fixed. Table 3.2 shows the possible configuration where U and D stand for uplink respectively downlink transmission and S is stated for reserved sub frames.

3.3.2 Slot structure

Each transmitted slot can physically be seen as a time frequency grid, where each resource element (RE) matches one OFDM sub carrier during OFDM symbol interval. The transmission bandwidth gives the number of sub carriers used for the transmission. LTE has two lengths of CP specified a normal and extended one. For normal CP, each slot has seven OFDM symbols and for extended six OFDM symbols are placed in each slot. The difference and the benefits of different

Configuration	Periodicity	Sub frame number									
		0	1	2	3	4	5	6	7	8	9
0	5 ms	D	S	U	U	U	D	S	U	U	U
1	5 ms	D	S	U	U	D	D	S	U	U	D
2	5 ms	D	S	U	D	D	D	S	U	D	D
3	10 ms	D	S	U	U	U	D	D	D	D	D
4	10 ms	D	S	U	U	D	D	D	D	D	D
5	10 ms	D	S	U	D	D	D	D	D	D	D
6	5 ms	D	S	U	U	U	D	S	U	U	D

Table 3.2: LTE frame type 2 uplink downlink configurations

lengths of CP will be discussed in Chapter 3.3.3.

In LTE downlink transmission the subcarrier spacing is 15 kHz. Hence these 12 subcarriers are grouped together to one resource block (RB) in frequency domain. Each RB uses 180 kHz bandwidth in one slot duration. For normal CP, each RB has 84 RE's, and for the extended CP the number is 74, due the longer CP length. Figure 3.5 shows RB structure of one slot length 0.5 ms for normal CP length [36].

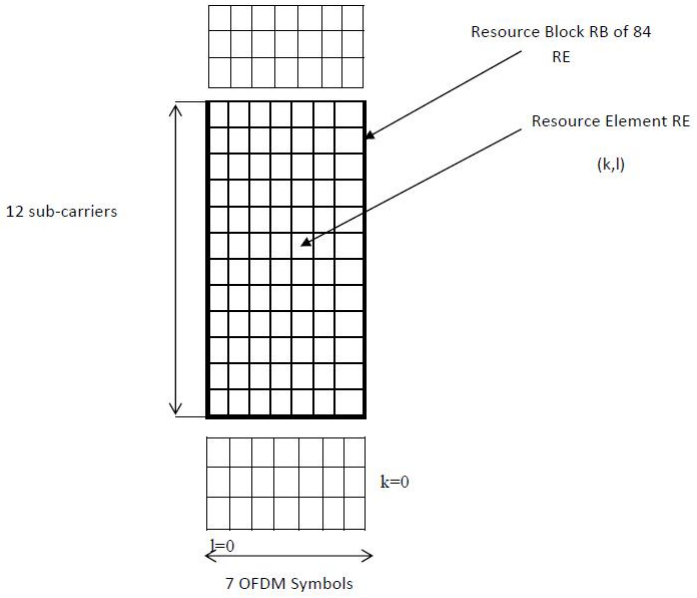

Figure 3.5: LTE resource grid for normal CP

3.3.3 Cyclic prefix

As already mentioned in Chapter 3.3.2 the LTE standard defines two different lengths of CP. Figure 3.6 from [21] illustrates the time domain structure of LTE slot, where the difference between the two CP lengths can be seen. Figure also shows that in case of normal CP, the first OFDM symbols slot is larger than the remaining, therefore the 0.5 ms slot has to be completely filled due the fact that the basic time unit T_s (15360) is not dividable by seven symbols. The prefix lengths are definded as followed:

$T_{CP} = 160T_s = 5.1\mu s$ for the first symbol and $T_{CP} = 144T_s = 4.7\mu s$ for the remaining OFDM symbols

$T_{CP-e} = 512T_s = 16.7\mu s$

There are two reasons why LTE has defined two CP lenths:

- For very large cells less efficient longer CP can be advantageous over normal one, due the large delay spread. On the other hand, if the channel performance is limited more by noise than by signal corruption, it may not recover the losses in terms of reduced received signal energy.
- For multicast or broadcast transmissions, cyclic prefix not only covers the time dispersion, but it also used to distinguish the timing difference between the transmissions from the cells involved.

3.4 Modulation

As previously stated LTE uses digital modulation technique and due the orthogonality of the signal there is no intra cell interference. Because of this reason high order modulations like Quadrature Phase Shift Keying (QPSK) and Quadrature Amplitude Modulation (QAM) are used to modulate and demodulate the data transmitted. However high order modulations result higher PAPR and larger power amplifier back offs reducing the available transmission power. The next section discusses PAPR for QPSK and QAM modulations. Figure 3.7 shows constellation diagrams of modulations used in LTE [30].

PAPR is defined as the peak power within one OFDM symbol normalized by average signal power [34]. The value of PAPR is directly proportional to the number of subcarriers given in Equation (3.1)[48].

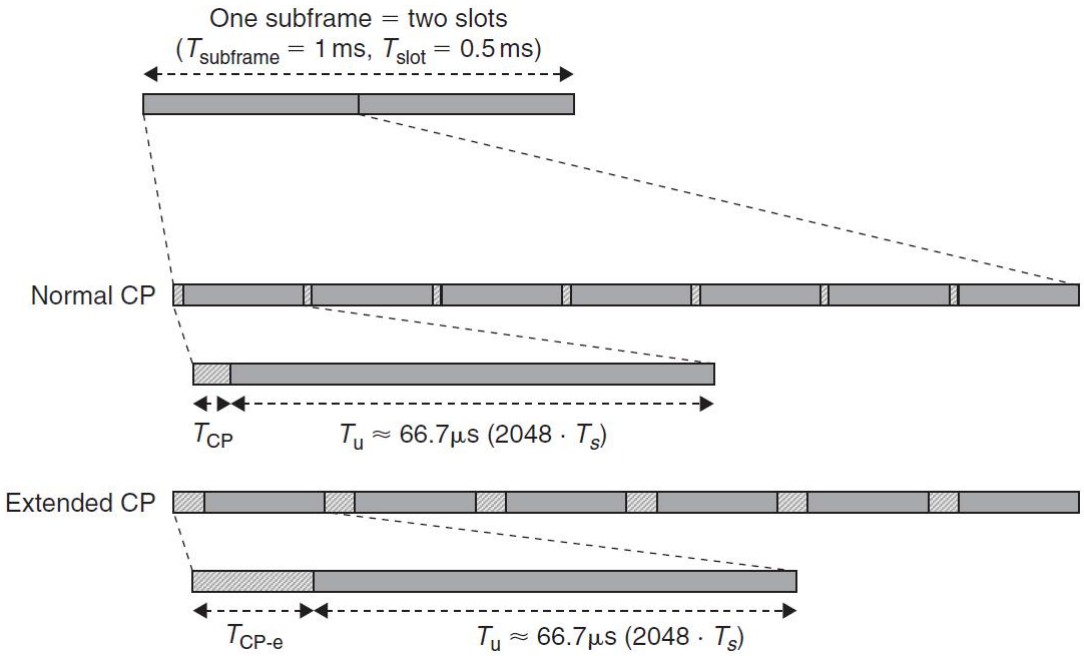

Figure 3.6: LTE time domain structure

$$PAPR(dB) \propto \log_{10} N \tag{3.1}$$

where

N is is the number of subcarriers

Large PAPR signal need high linear power amplifiers to avoid modulation distortion, hence they have to operate with large back off from their peak power which results low power efficiency [38].

3.4.1 QPSK, 16-QAM and 64-QAM

In QPSK the modulation alphabet consists of four different signaling choices, where a pair of two consecutive bits is converted from serial to parallel and then mapped into its complex value constellation [39] as seen Figure 3.8. With QPSK up to two bits of information can be transmitted during each modulation symbol interval. Assuming maximum amplitude A in both real and imaginary axis and unit average power, A can be calculated as follows [33]:

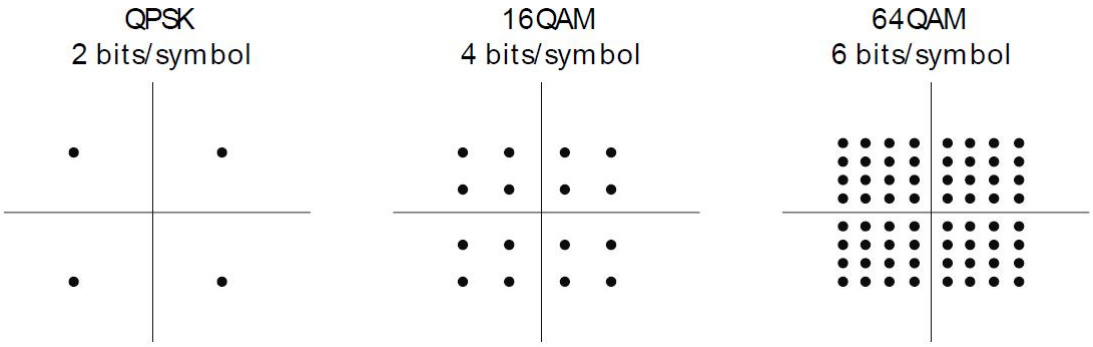

Figure 3.7: LTE modulation constellations

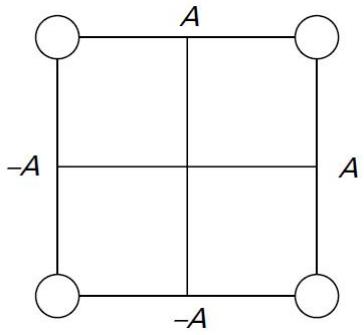

Figure 3.8: QPSK constallation

$$\frac{4(A^2 + A^2)}{4} = 1$$
$$\Rightarrow A = \frac{1}{\sqrt{2}} \tag{3.2}$$

All the constellation points have the same power so PAPR can be calculated as shown:

$$PAPR_{QPSK} = \frac{A^2 + A^2}{1} = 1 = 0dB \tag{3.3}$$

This result can be seen as a constant envelope signal.

Higher modulation like 16-QAM gives 16 different alternatives (four bits per symbol), which allows up to four bits of information to be transmitted, therefore it is more bandwidth efficient and permits higher data rates than QPSK. Figure 3.9 shows the constellation diagram in two dimensional plane and again assuming unit average power the components can take amplitude values of $3A$, A, $-A$ and $-3A$, where A can be expressed as follows:

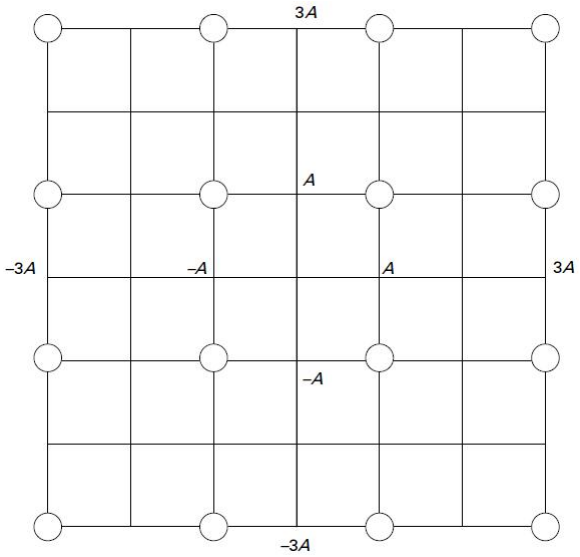

Figure 3.9: 16-QAM constallation

$$\frac{4(A^2 + A^2 + A^2 + 9A^2 + A^2 + 9A^2 + 9A^2 + 9A^2)}{16} = 1$$
$$\Rightarrow A = \frac{1}{\sqrt{10}} \tag{3.4}$$

And the maximum PAPR:

$$PAPR_{16-QAM} = \frac{9A^2 + 9A^2}{1} = 1.8 = 2.55dB \tag{3.5}$$

This means 16-QAM has a maximum PAPR of 2.55 dB with 25 % probability for the four outer corner symbols. To obtain PAPR for four inner symbols is similar to equation (3.3), but for different A value:

$$PAPR_{16-QAM} = \frac{A^2 + A^2}{1} = 0.2 = -7dB \tag{3.6}$$

And PAPR for the remaining eight constallation points:

$$PAPR_{16-QAM} = \frac{A^2 + 9A^2}{1} = 1 = 0dB \tag{3.7}$$

In case of 64-QAM one have logically 64 different choices (constellation points) shown in Figure 3.10. It maps six bit per symbol, hence it has three times larger capacity than QPSK. This modulation scheme is used in systems like 802.11 a/g. Again unit power is assumed and the amplitude values are $7A$, $5A$, $3A$, A, $-A$, $-3A$, $-5A$ and $-7A$ and A is given using the same calculation method:

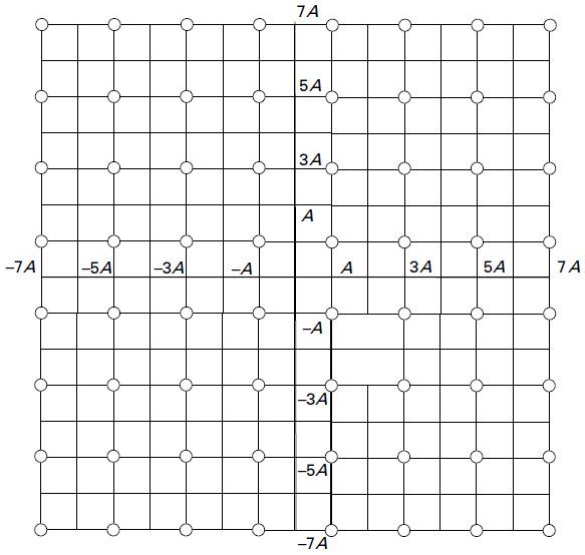

Figure 3.10: 64-QAM constallation

$$A = \frac{1}{\sqrt{42}} \tag{3.8}$$

And the maximum PAPR:

$$PAPR_{64-QAM} = \frac{49A^2 + 49A^2}{1} = \frac{98}{42} = 3.68dB \tag{3.9}$$

Meaning the four outer symbols result a PAPR of 3.68 dB with 6.25 % (1/16) probability.

3.4.2 Pilot structure

One of the central problems in OFDM transmission is how to be able to track and estimate multipath propagation environments. This is solved by putting reference symbols also known as pilots in to the transmitted data. These symbols are known to both transmitter and receiver; hence they are carrying no data and are applied for proper channel estimation for each subcarrier. In LTE three types of reference signals are used [21]. Figure 3.11 illustrates the idea of inserted reference signals in two slots for cell specific reference symbols.

- Cell specific reference signals
- UE specific reference signals
- Broadcast reference signal

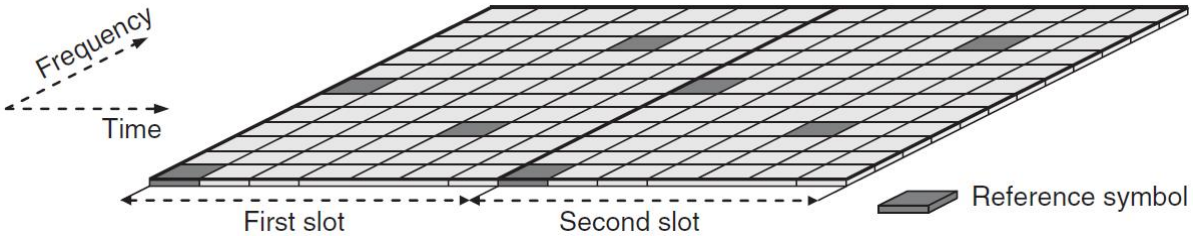

Figure 3.11: Structure of cell specific reference symbols

There are three main general uses for the reference symbols used in LTE [4]:

- Measuring the channel quality
- Channel estimation
- Initial acquisition and cell search

In the next chapter channel estimation will be discussed, since the reference symbols are mainly used for channel estimation in the LTE simulation model used for this Thesis.

3.4.3 Channel estimation

Channel estimation is important part of LTE receiver design, since in order to recover the transmitted information correctly, one need to know, how the channel conditions are changed over time. The estimation of the channel effects is based on an approximate underlying model of radio propagation channel [31]. There are different channel estimation approaches used for pilot based estimation like Least Square (LS), Minimum Mean Square (MMSE) and Least Mean Square (LMS). This work describes the MMSE estimator, which is used in the MATLAB simulator model used in this thesis.

Generally OFDM transmission can be written in form of:

$$y = XFh + n \tag{3.10}$$

where

y is the received signal

X is diagonal matrix with data, reference symbols or zeros

F is FFT matrix

h is channel impulse response to be estimated

n is white Gaussian noise

Using the method described in [47] the Channel Impulse Response (CIR) can be calculated in equation (3.11), where they take advantage of auto covariance and the cross covariance matrixes of the reference symbols.

$$\hat{h} = R_{hY_r} R_{Y_r Y_r}^{-1} Y_r \tag{3.11}$$

where

$\hat{h}$ is estimated CIR

Y_r is received reference symbols without data or zeros

R_{hY_r} is cross covariance matrix of h and Y_r

$R_{Y_rY_r}$ is auto covariance matrix of Y_r

The covariance matrixes are calculated according to eqations (3.12) to (3.15) [36]. For auto covariance matrix:

$$\begin{aligned} R_{Y_rY_r} &= E[Y_rY_r^H] && (3.12)\\ &= E[(X_rF_rh+n_r)(X_rF_rh+n_r)^H] \\ &= E[(X_rF_rh+n_r)(X_r^HF_r^Hh^H+n_r^H)] \\ &= X_rF_rE[hh^H]X_r^HF_r^H + E[n_rn_r^H] + X_rF_r[hn_r^H] + [n_rh^H]X_r^HF_r^H \\ &= X_rF_rR_{hh}X_r^HF_r^H + \sigma_n^2I_{n_r} && (3.13) \end{aligned}$$

and for the cross covariance matrix:

$$\begin{aligned} R_{hY_r} &= E[hY_r^H] && (3.14)\\ &= E[hh^HX_r^HF_r^H + n_rh^HX_r^HF_r^H] \\ &= R_{hh}X_r^HF_r^H \\ &= X_r^HF_r^h && (3.15) \end{aligned}$$

Putting it all into equation (3.11) CIR can be calculated as shown:

$$\hat{h} = X_r^HF_r^H(X_rF_rR_{hh}X_r^HF_r^H + \sigma_n^2I_{n_r})^(-1)Y_r \qquad (3.16)$$

3.5 Link adaptation

Basically there are two types of link adaptation, power and rate control. Power control has been used in CDMA based mobile communication systems such as WCDMA. A variable transmit power is used to compensate the channel quality variations. The goal of power control is to maintain constant data rate at the receiver. Basically transmit power is increased when the channel quality decreases and vice versa if the conditions become more advantageous, so the transmit power is inversely proportional to channel quality conditions as seen in Figure 3.12 (a).

On the other hand in packet switched mobile communication services constant data rate is not necessary needed, in many cases there is a need for rate as high as possible and this is the case where the modulation and coding rate is varied depending on the channel conditions. This technique is called Adaptive Modulation and Coding (AMC). Short term data variations can be tolerated as long as the average data rate remains constant, which is achieved by rate control seen in Figure 3.12 (b)[21]. It can be shown that rate control is more efficient than power control therefore AMC is used in simulator written for this thesis and described in detail below[28] and[26].

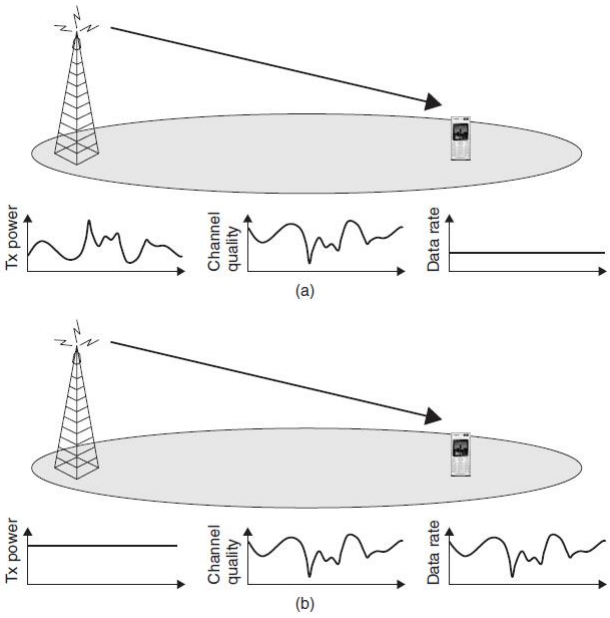

Figure 3.12: (a) Power control (b) rate control

3.5.1 Adaptive Modulation and Coding

In general the receiver chooses the best modulation and coding rate according to the channel quality response from receiver via Channel Quality Indicator (CQI). In downlink eNodeB can select between QPSK, 16-QAM and 64-QAM and possible coding rates listed in Table 5.4. There are basically two degrees of freedom for AMC [46]:

- **Modulaton Scheme:** Low order modulation e.g. QPSK are more robust to poor channel conditions, but gives a lower transmission rate. On the

other hand e.g. 16-QAM provides better transmission rate however is more vulnerable to channel conditions.

- **Coding Rate:** For given modulation different coding rates can be chosen from Table 5.4. Lower coding rates are used for poorer channel conditions and vice versa.

The reported CQI is calculated from pilot tones used in downlink transmission described in Chapter 3.4.2. The CQI, best Modulation and Coding Scheme (MCS), reported by UE is based on the Block Error Rate (BLER) probability not exceeding 10 %. Simple method for UE to calculate best possible MCS can be based on a BLER thresholds as seen in Figure 3.13. The UE selects the best CQI that satisfies the condition $BLER \leq 10^{-1}$. Optimal switching points betweend modulation order and coding rates depend on may different factors like Quality of Service (QoS) and cell throughput [46].

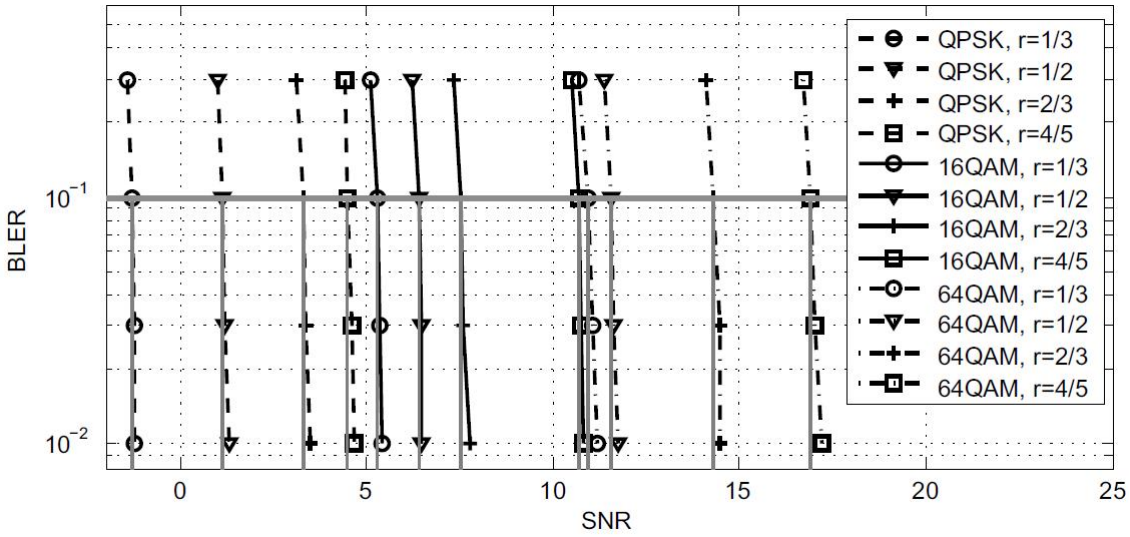

Figure 3.13: CQI Threshold example $BLER \leq 10^{-1}$

3.6 MIMO

Multiple input multiple output (MIMO) is one of the central technologies used in LTE to improve coverage, capacity, Quality of Service (QoS) and specified data rates. It is a very large topic and this thesis describes only the basics of it. For more detailed information please see the references used in this chapter e.g [18].

MIMO operation includes techniques like spatial multiplexing, pre-coding and transmit diversity which fundamentals will be discussed in this chapter.

3.6.1 Basics

The basic principles of MIMO as shown in Figure 3.14, where different data streams are transferred through pre-coder followed by signal mapping and OFDM signal generation [30].

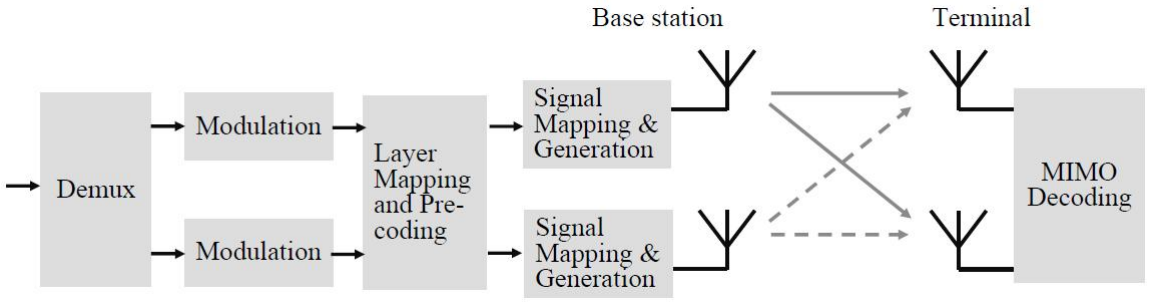

Figure 3.14: MIMO principle

The receiver antennas need to be able to separate the transmitted streams, therefore reference symbols are used to separate them, where they are altered between antennas. For LTE standard 3GPP has specified to cover up to four transmission and reception antennas, hence as the number of antennas increases the needed SNR increases with the drawback of transmitter/receivers complexity as well as the reference symbol overhead.

3.6.2 Spatial multiplexing

With MIMO technique an additional dimension to time and frequency is introduced named spatial dimension, which allows achieving the required peak data rates LTE has specified. Data streams can be transmitted over different parallel channels using the same bandwidth and no additional power. The capacity is linearly related to the number of transmitter/receiver antenna pair.

The simultaneously transmitted bit streams cause interference at the receiver; hence different interference cancelling techniques are used at the receiver, e.g. MMSE as described in Chapter 3.4.3. Figure 3.15 gives an example of 2x2 MIMO transmission, where the received signal can be written as stated in eqation (3.17) [21].

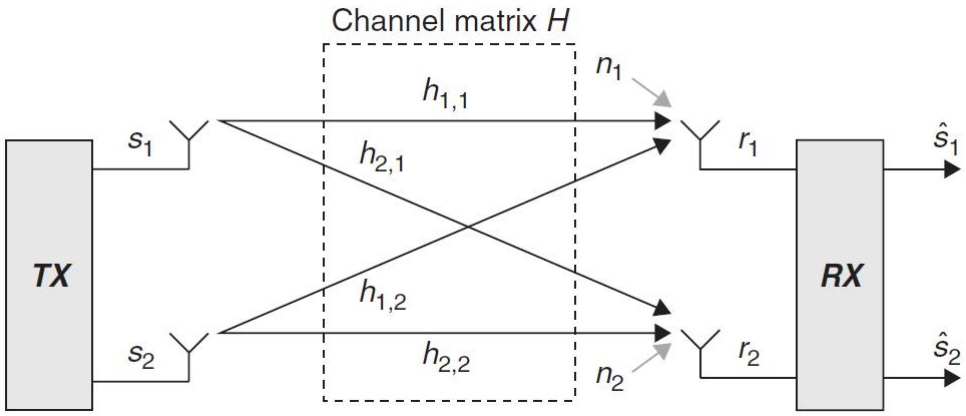

Figure 3.15: MIMO 2x2 example

Now the received signal r can be expressed in matrix form as:

$$r = \begin{bmatrix} r_0 \\ r_1 \end{bmatrix} = \begin{bmatrix} h_{1,1} & h_{1,2} \\ h_{2,1} & h_{2,2} \end{bmatrix} \begin{bmatrix} s_1 \\ s_2 \end{bmatrix} + \begin{bmatrix} n_1 \\ n_2 \end{bmatrix} = Hs + n \tag{3.17}$$

where

H is 2x2 channel matrix

s is transmitted symbols

n is white Gaussian noise

Assuming no noise the transmitted symbols s_k can be obtained at the receiver side as follows:

$$s = \begin{bmatrix} s_0 \\ s_1 \end{bmatrix} = \frac{1}{h_{1,1}h_{2,2} - h1,2h2,1} \begin{bmatrix} h_{1,1} & -h_{1,2} \\ -h_{2,1} & h_{2,2} \end{bmatrix} \begin{bmatrix} r_1 \\ r_2 \end{bmatrix} \tag{3.18}$$

3.6.3 Pre-coding

The basic idea in pre-coding is giving the transmitted signal from different antennas different weights in order to maximize the SNR at the receiver. The

transmitter needs to know from the receiver about the channel conditions and for large MIMO systems this increases the overhead.

In open loop MIMO systems as the LTE simulator used in this work, one can use a set of pre-coding matrixes, which is known for both transmitter and receiver. This set of matrixes is also called MIMO codebook and noted as P, where $L = 2^r$ is the size of it and r is the number of feedback bits needed for to index the codebook [33]. After the MIMO system is specified with a codebook, the receiver observes the channel conditions and selects the best pre-coding matrix for that condition. The Pre-coding Matrix Index (PMI) is then reported back to the transmitter as illustrated in Figure 3.16.

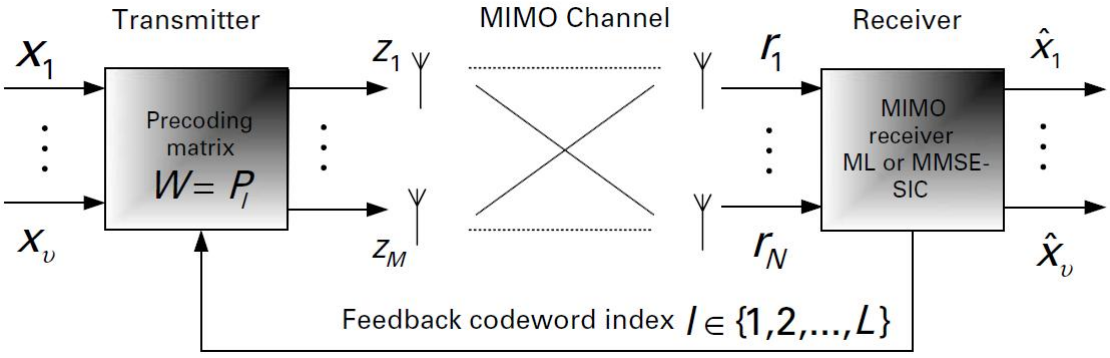

Figure 3.16: Closed loop MIMO system

An example of pre-coding matrixes for two antenna ports is described beneath, since LTE simualtor for this work uses the same codebook as described in [33]. For the two antenna port pre-coding a grouping of 2x2 identity matrix and DFT matrix is used, which for two antenna ports is described as follows:

$$W = \frac{1}{\sqrt{2}} \begin{bmatrix} 1 & 1 \\ 1 & e^{j\pi} \end{bmatrix} = \frac{1}{\sqrt{2}} \begin{bmatrix} 1 & 1 \\ 1 & -1 \end{bmatrix} \tag{3.19}$$

By introducing a shift parameter $\frac{g}{G}$ the Fourier matrix can be written as follows:

$$W_g = e^{j\frac{2\pi m}{N}(n+\frac{g}{G})} \qquad m, n = 0, 1, \ldots (N-1) \tag{3.20}$$

Now a set of four 2x2 Fourier matrices can be defined for $G = 4$ and $g = \{0, 1, 2, 3\}$:

$$W_0 = \frac{1}{\sqrt{2}} \begin{bmatrix} 1 & 1 \\ 1 & -1 \end{bmatrix} \tag{3.21}$$

$$W_1 = \frac{1}{\sqrt{2}} \begin{bmatrix} 1 & 1 \\ \frac{1+j}{\sqrt{2}} & \frac{-1-j}{\sqrt{2}} \end{bmatrix} \tag{3.22}$$

$$W_2 = \frac{1}{\sqrt{2}} \begin{bmatrix} 1 & 1 \\ j & -j \end{bmatrix} \tag{3.23}$$

$$W_3 = \frac{1}{\sqrt{2}} \begin{bmatrix} 1 & 1 \\ \frac{-1+j}{\sqrt{2}} & \frac{1-j}{\sqrt{2}} \end{bmatrix} \tag{3.24}$$

In LTE, the codebook for two antenna ports includes seven different code words, four rank 1 and three for rank 2, which are summarized in Table 3.3 [7]. Rank 1 code words are just columns of rank 2 code words. The idea to limit the codebook alphabet only to $\{1, j\}$ was to reduce the complexity of the UE in calculating the Channel Quality Indicator (CQI) by avoiding matrix calculations.

Codebook index	Number of layers	
	$\upsilon = 1$	$\upsilon = 2$
0	$\frac{1}{\sqrt{2}} \begin{bmatrix} 1 \\ 1 \end{bmatrix}$	$\frac{1}{\sqrt{2}} \begin{bmatrix} 1 & 0 \\ 0 & 1 \end{bmatrix}$
1	$\frac{1}{\sqrt{2}} \begin{bmatrix} 1 \\ -1 \end{bmatrix}$	$\frac{1}{2} \begin{bmatrix} 1 & 1 \\ 1 & -1 \end{bmatrix}$
2	$\frac{1}{\sqrt{2}} \begin{bmatrix} 1 \\ j \end{bmatrix}$	$\frac{1}{2} \begin{bmatrix} 1 & 1 \\ j & -j \end{bmatrix}$
3	$\frac{1}{\sqrt{2}} \begin{bmatrix} 1 \\ -j \end{bmatrix}$	-

Table 3.3: LTE MIMO two antenna port codebook

3.6.4 Transmit diversity

Transmit diversity is basically sending multiple copies of the same signal in order to exploit the gains from independent fading between the antennas. It is common in downlink cellular systems; therefore it is cheap and easy to install more antennas at the base station than to modify single UE, which may vary from manufacturer to manufacturer. On the other hand in LTE because of the short transmission time of one sub-frame (1 ms), there is little time diversity available.

It can be exploited using Hybrid Automatic Repeat Request (HARQ) Protocol, which will be discussed in detail in Chapter 3.7. In the standardization phase of LTE many transmit diversity schemes were discussed and evaluated, for detailed view of the different techniques reader is adviced to see [33] Chapter 6.1.

To sum up the previously mentioned source, during the standardization and evaluation phase in LTE there was a debate between two different time diversity techniques Cyclic Delay Diversity (CDD) [46] and block code based schemes such as Alamounti space time coding [16]. CDD has a drawback with perfectly correlated antennas where there is no diversity available and block code based schemes do not scale with the number of antennas, where the performance is penalized [33].

After long discussion the decision was made for block codes and for two antenna ports Space Frequency Block Coding (SFBC) was specified as a standard. For further information see [40] and [32].

3.7 Multicodeword-MIMO HARQ

The basic idea behind ARQ is that the terminal may rapidly request a retransmission if a transmission has been decoded with errors. In addition, HARQ provides a tool for rate adaption [21]. The difference between ARQ and HARQ protocol is that HARQ is a combination of Forward Error Coding (FEC) and error detection. ARQ protocol only uses the error detection method. It is also to be noted, that HARQ protocol is a function spread over both physical and MAC layer. MAC layer control the HARQ entity, where the combination and other bit operations are done by the physical layer.

3.7.1 ARQ protocol categories

Different types ARQ protocols can be divided into three categories:

- *Stop-and-wait* which is the simplest type of ARQ scheme. The transmitter waits after sending a packet for an acknowledgment (ACK) or a negative acknowledgement (NACK) from receiver and then sends either a new packet, after receiving ACK or the same packet in case of NACK. Drawback of this method is the long waiting time at the transmitter waiting for ACK/NACK.
- *Go-back-N* has a defined window size where packets are sent without waiting for an ACK. When NACK is received the transmitter starts to retransmit packets from the missing packet, which in other words means, that possible

correctly decoded packets, after sending the missing packet for the first time, are simply ignored and retransmitted again. This is also the biggest drawback of Go-back-N, because of the duplicate transmissions of the same data.

- *Selective repeat protocols* can handle this problem and keeps sending the packets in defined window size. After receiving an NACK the protocol continues sending new packets and tries to resend only the corrupted one, therefore it has the best performance from the categories.

Since LTE has a modified implementation of Stop-and-wait protocol it will be discussed in detail. Figure 3.17 illustrates how the protocol works for one transmission process. As seen in the illustration the problem is the long waiting time, where the transmitter is idle waiting for ACK/NACK report. On the other hand the receiver only has to buffer one packet at the time that is currently being decoded.

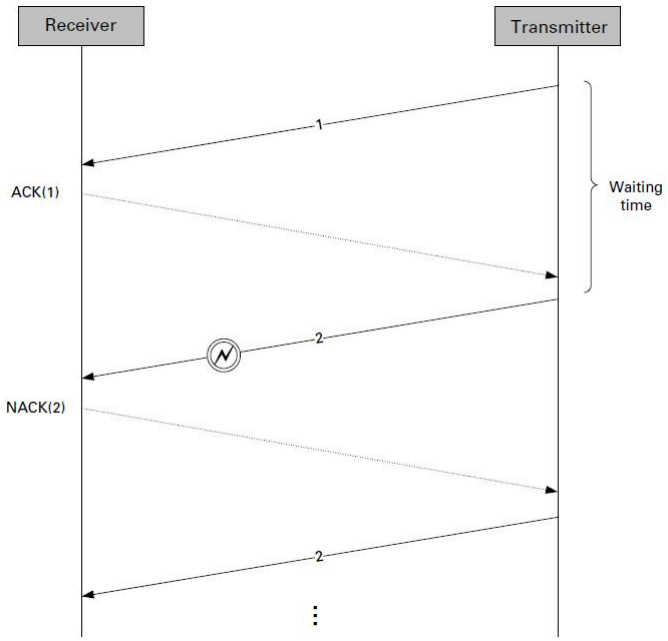

Figure 3.17: ARQ stop-and-wait protocol

LTE uses multiple parallel Stop-and-wait processes. In standard eight parallel processes are specified see equation (3.25). After receiving a transport block transmitter tries to decode the block and informs transmitter with an information bit if block number was successfully decoded respectively not. Additionally

transmitter needs to know which block was not correctly received; this is solved by the timing of the acknowledgement to allocate which process belongs to which transport block. The multiple parallel HARQ process is shown in Figure 3.18 from [21]. As seen transport block number 5 was successfully decoded before transport block 1, which had to be retransmitted two times. The data is not in sequence, but the ordering is done in the upper Radio Link Control (RLC) layer.

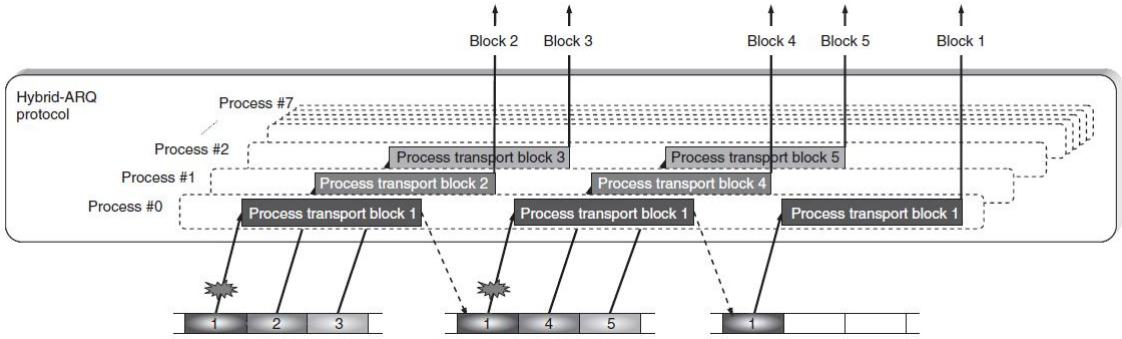

Figure 3.18: Multiple parallel processes

The number of HARQ processes can be calculated in equation (3.25) [33].

$$N_{HARQ} = \left\lceil \frac{2T_p + T_{sb} + T_{uep} + T_{ACK} + T_{nbp}}{T_{sb}} \right\rceil \tag{3.25}$$

where

N_{HARQ} is the number of HARQ processes

T_p is propagation time between UE and eNodeB

T_{sb} is subblock (SB) transmission time

T_{uep} is UE processing time including decoding

T_{nbp} is eNodeB processing time

The parameters are illustrated in the Figure 3.19 where and values are listed in the Table 3.4

Now the number of HARQ processes in LTE can be calculated using the equation (3.25) and Table 3.4

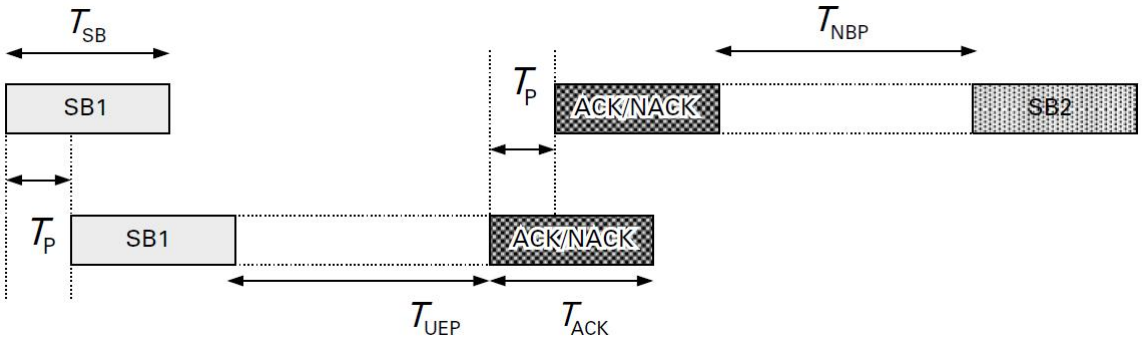

Figure 3.19: Stop-and-wait HARQ round trip time (RTT)

Parameter	Symbol	Value
Propagation time	T_p	Neglible
Sunbblock transmission time	T_{sb}	1 ms
UE processing time	T_{uep}	3 ms
ACK transmission time	T_{ACK}	1 ms
eNodeB processing time	T_{nbp}	3 ms

Table 3.4: LTE HARQ RTT paremeters

$$N_{HARQ} = \left\lceil \frac{0+1+3+1+3}{1} \right\rceil = 8 \tag{3.26}$$

In LTE the erroneously decoded blocks are kept at the receiver's buffer, hence the partly available data can be used with the retransmitted packet. HARQ scheme support so called Chase combining and incremental redundancy methods to deal with the retransmission at the receiver's side. These methods will be discussed in Chapter 3.7.2.

HARQ protocols can be characterized in synchronous vs. asynchronous and flexible vs. non flexible depending on the resource usage and link adaptation [21].

Asynchronous retransmission can occur at any time, whereas synchronous retransmissions happen at certain fixed time after previous transmission. Therefore asynchronous protocol has more flexibility, but the usage of synchronous retransmission does not require any explicit HARQ process number signaling as the information can be extracted from the sub frame number.

The adaptive protocol takes the frequency resources into account, where more suitable transmission format can be selected. Non adaptive protocol on the other

hand uses the same frequency resources as the same transmission format as the initial transmission.

3.7.2 Chase Combining and Incremental Redundancy

The simplest form of HARQ scheme was proposed by Chase in 1985 [19]. It can be seen as additional repetition coding, since no new redundancy is transmitted. At each retransmission exact copy of the information bits are transmitted and combined at the receiver using maximum ratio combining. Chase combining does not give additional coding gain, it only increases the received $\frac{E_b}{N_0}$ for each retransmission, where E_b is energy over bit and N_0 spectral noise density. For further details about $\frac{E_b}{N_0}$ see [41]. Figure 3.20 from [21] shows an example of using Chase combining.

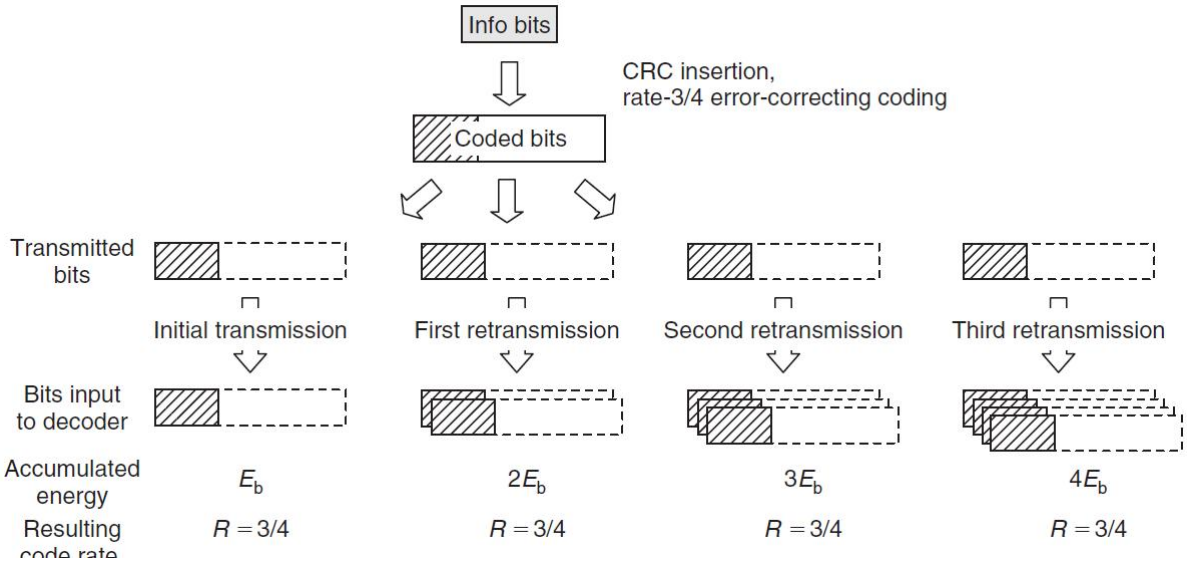

Figure 3.20: Example of Chase combining

In case of Incremental redundancy (IR) the retransmission bit do not have to be the same then different sets of coded bits are transmitted each having the same amount of information bits [44]. In case of retransmission different set of bits from previous transmission are sent, combined and sent to decoder. Retransmission bits do not necessarily need to have the same modulation scheme as the previous. With IR low rate coding is often used and the different retransmission set of bits are generated by puncturing the encoder output bits. Figure 3.21 from [21] shows an example with a 1/4 code rate, where at the first retransmission every third

coded bit is sent at rate 3/4. In case of decoding error a new set of bits is created giving a rate of 3/8. After second retransmission the rate will be 1/4 and for any further retransmission the information bits will be repeated. IR not only gives a gain in $\frac{E_b}{N_0}$, but it also achieves a coding gain for each retransmission.

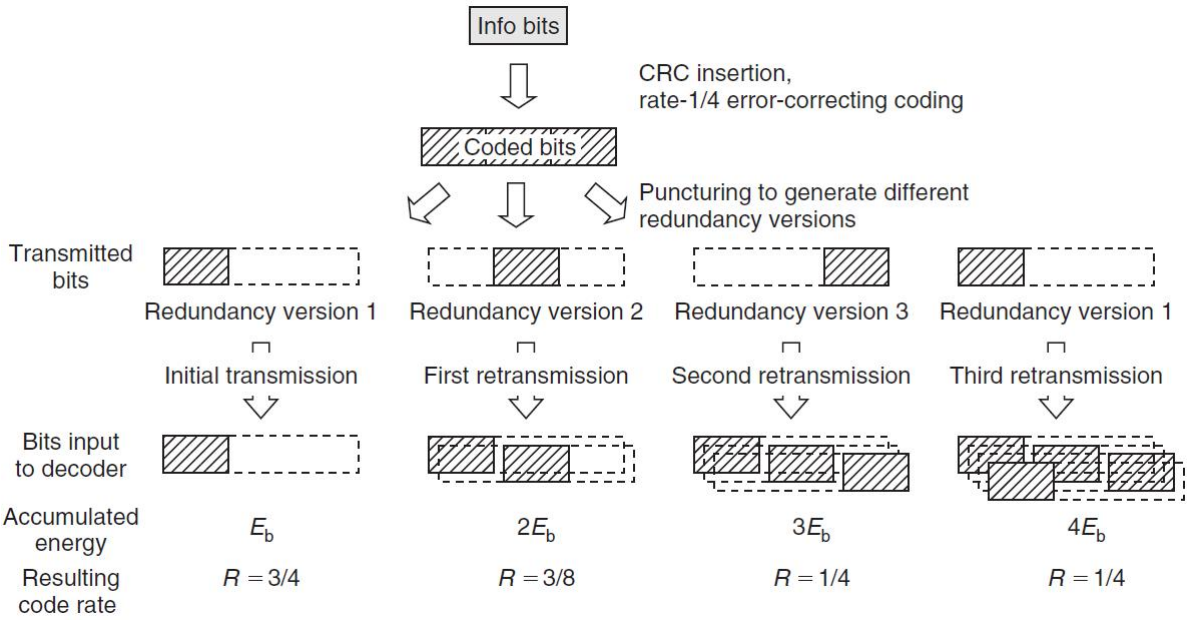

Figure 3.21: Example of Incremental redudancy

Comparison of Chase and IR shows that IR achieves a larger gain at higher initial coding rates while for lower rates both techniques are more or less equal [20]. Moreover the performance gain of IR compared to Chase combining can also depend on the relative power difference between the transmission attempts [24].

3.7.3 Multicodeword-MIMO HARQ alternatives

In LTE three different retransmission schemes were discussed [3], which performance is the main scope of this thesis and discussed in detail in the next chapters:

- Independent processes
- Blanking
- Non-blanking

3.7.3.1 Independent

Independent HARQ process means in case of two antenna ports that both are having their own HARQ process and are working totally independent from each other. Table 3.5 shows an example of two independent processes for two antennas A and B. Each antenna gets their own ACK/NACK for the transmitted codeword and retransmit it in case of NACK.

Antenna A	A_1	NACK	A_1	ACK	A_2	ACK	A_3	NACK	A_3	ACK	A_4
Antenna B	B_1	ACK	B_2	ACK	B_3	NACK	B_3	NACK	B_3	ACK	B_4

Table 3.5: Independent HARQ transmission example

Codewords A_k and B_n are transmitted independently and in every time slot both antennas are sending a codeword to the receiver. This transmission scheme has the best performance compared to the next two, but there is hardly any literature about the performance difference compared to the other schemes except in [3], where blanking method is shown as being the worst in terms of throughput. The comparison of these three HARQ cases is the main topic of this thesis.

3.7.3.2 Blanking

In this transmission scheme there is only one HARQ process but two ACK/NACK for two antennas. Table 3.6 shows an example transmission.

Antenna A	A_1	NACK	A_1	ACK	A_2	ACK		ACK	A_3	ACK	A_4
Antenna B	B_1	ACK		ACK	B_2	NACK	B_2	ACK	B_3	ACK	B_4

Table 3.6: Blanking HARQ transmission example

As seen in the table, if one packet is correctly decoded and the other one not, only the erroneously decoded codeword is resent (A_1) and the other antennas codeword is left blank (no B_2). This makes it more probable for the sent codeword to arrive correctly at the transmitter, since there is no other message to interfere with the data.

3.7.3.3 Non-blanking

In last non-blanking transmission scheme there is only one ACK/NACK for two codewords. Again a transmission example is shown in Table 3.7.

Antenna A	A_1	n	A_1	a	A_2	a	A_2	a	A_2	a	A_3
		NACK		ACK		NACK		NACK		ACK	
Antenna B	B_1	a	B_1	a	B_2	n	B_2	n	B_2	a	B_3

Table 3.7: Non-blanking HARQ transmission example

The n and a indicates that codeword from that antenna was decoded correctly, but since there is only one ACK/NACK and only one codeword has been decoded correctly, the transmitter gets a NACK and resends both messages again and does not leave empty (blank) spaces in order the get the erroneously decoded codeword higher probability to get through. This is seen in the example tables where in blanking transmission scheme B_2 does not get interfered by antenna A and needs only be retransmitted one, where in non-blanking scheme B_2 has to be sent three times.

Chapter 4

LTE Downlink

This chapter discusses the functions of the different layers in LTE downlink, where data is sent from base station to the mobile terminal. Figure 4.1 illustrates the LTE layer structure [21]. The simulator used in this work has only the two lowest layers implemented; nevertheless this chapter will discuss also the third layer named Radio Link Control (RLC) briefly to give the reader a better overview of the functionality.

Then more on detailed view of layer 2 the Medium Access Control (MAC) will follow including multiplexing and mapping different channels to communicate with the lowest layer the Physical Layer (PHY). MAC layers other functionalites like scheduling and discontinuous reception are also reviewed as well as the main focus of this thesis the HARQ entity, which is split over MAC and PHY layers.

Moving further to lowest layer the Physical Layer its important functions like channel coding with Cyclic Redundancy Check (CRC) and turbo coding are discussed. Nevertheless OFDM modulation is revised and finally HARQ functions at the PHY layer level are described.

4.1 RLC Layer

RLC is located between Packet Data Convergence Protocol (PDCP) and MAC layer and it communicates with the upper one using Service Access Point (SAP) and with the lower one via logical channels. RLC is responsible for segmentation of RLC Protocol Data Units (PDU) from PDCP into Service Data Units (SDU) suitable size for MAC layer as shown in Figure 4.2 from [21].

RLC is also responsible for retransmission of wrongly received PDUs and remov-

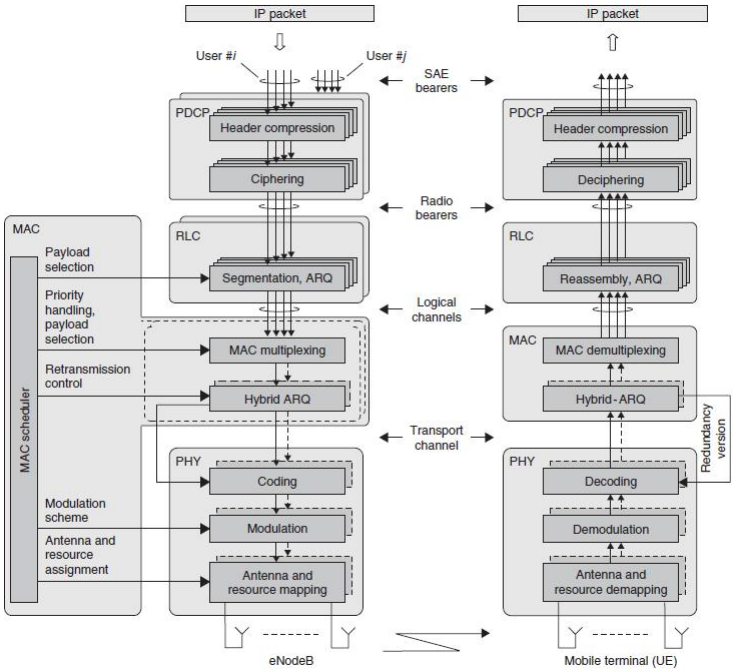

Figure 4.1: LTE downlink architecture

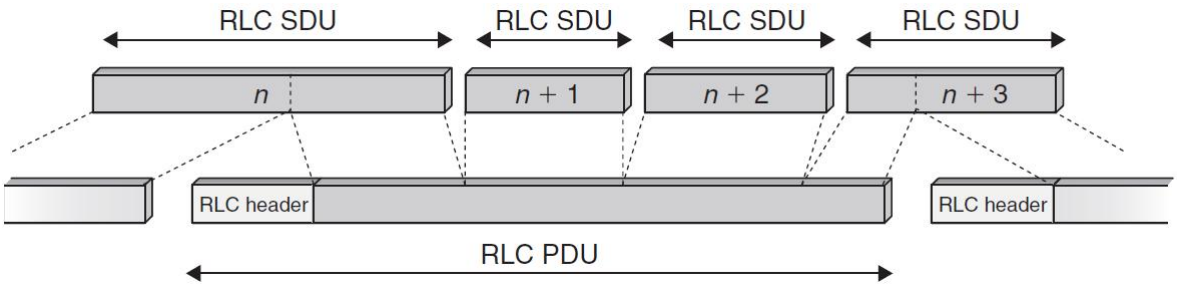

Figure 4.2: RLC PDU to SDU segmentation

ing the duplicate ones. Hence it manages the in sequence delivery of SDUs for the upper layers. The functions of RLC are performed by RLC entities, which can be configured in three different modes:

- Transparent Mode
- Unacknowledged Mode
- Acknowledged Mode

For further details to RLC Layer functionality reader is adviced to see [46].

4.2 MAC Layer

MAC layer is the second lowest layer in the LTE architecture and communicates with RLC through logical channels and with physical layer through transport channels; therefore it performs multiplexing and demultiplexing between those channels. Figure 4.3 from [46] gives an overview about the MAC layer functions, hence it can be considered as a controller with multiplexing and HARQ entity.

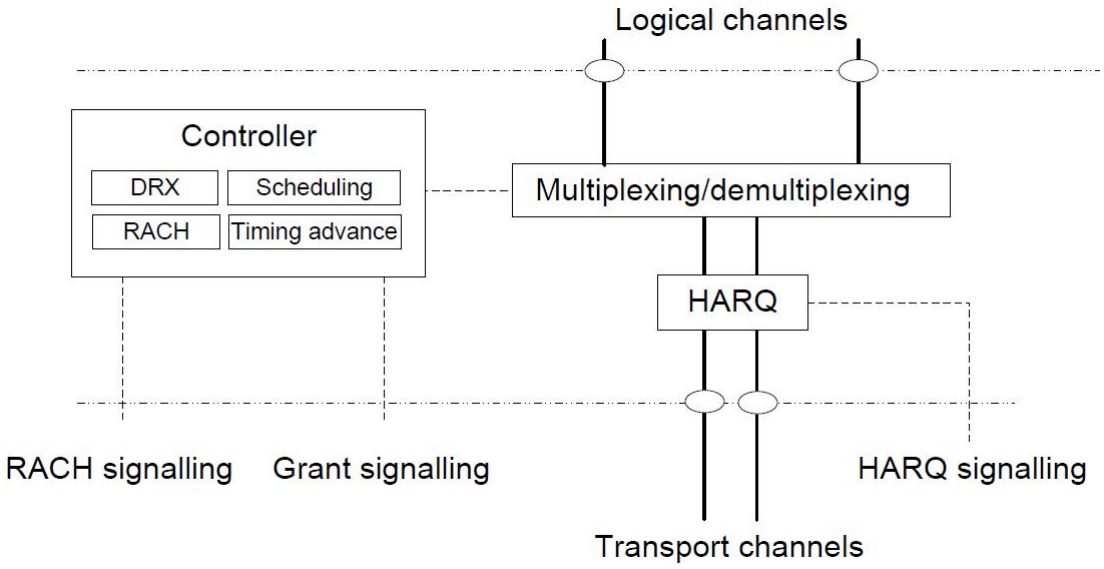

Figure 4.3: Overview of LTE MAC layer

4.2.1 Multiplexing and mapping

As already stated above MAC layer communicates with logical and transport channels which need to be mapped correctly when transferring to other layers. Following logical channels for downlink are specified for LTE [9]:

- *Broadcast Control Channel (BCCH)* which is used to broadcast system information.

- *Paging Control Channel (PCCH)* which notifies UEs of an incoming call or change of system information.
- *Common Control Channel (CCCH)* which delivers control information when there is no confirmed association between UE and the eNobeB.
- *Multicast Control Channel (MCCH)* which transmits control information related to reception of broadcasting information.
- *Dedicated Traffic Channel (DTCH)* which transmits dedicated user data.
- *Multicast Traffic Channel (MTCH)* which transmits user data of broadcast services.

On the other hand following transport channels in downlink direction are defined in [9]:

- *Broadcast Channel (BCH)* which is used to transport parts of system information for DL-SCH.
- *Downlink Shared Channel (DL-SCH)* which transport downlink user data or control messages.
- *Paging Channel (PCH)* which transports paging information to UEs.
- *Multicast Channel (MCH)* which transports user data or control messages related to multicasting or broadcasting.

Figure 4.4 illustrates the 3GPP specification of channel mapping und multiplexing in downlink direction. It can be seen that DL-SCH carries information from all the logical channels with exception of PCCH.

4.2.2 Scheduling

One of the basic principles of LTE is that time and frequency resources are dynamically shared between the users. Scheduler is in charge of assigning and controlling the resources. The signals used for scheduling are standardized by 3GPP, but the details are left for the eNodeB implementation. Basically a terminal listens to the scheduling commands received from a unique serving cell which every 1 ms TTI makes a scheduling decision and sends it to the UE. These commands include transport block size, modulation scheme, antenna mapping and logical channel multiplexing. Figure 4.5 from [21] shows the transport format selection

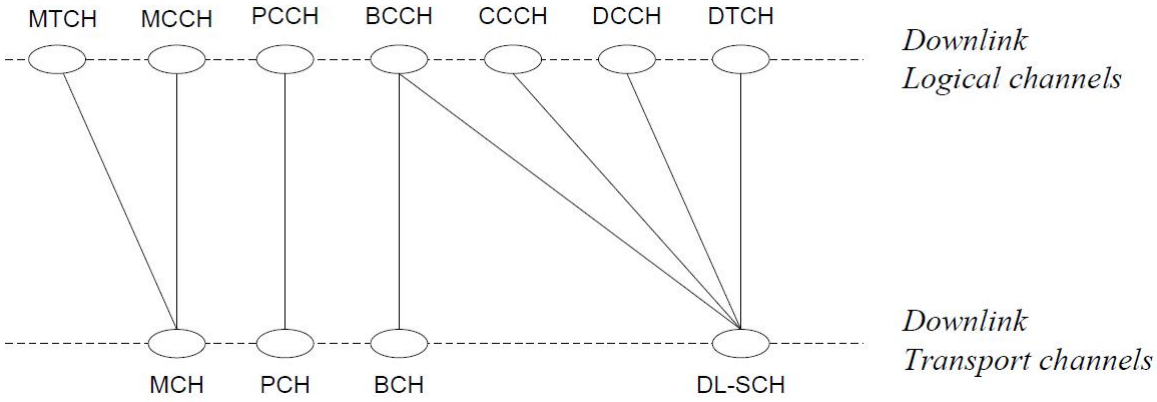

Figure 4.4: Downlink logical to transport channel mapping

in downlink transmission. The basic time frequency unit in scheduler is called a resource block which spans of 180 kHz and in each 1 ms those blocks are assigned to DL-SCH.

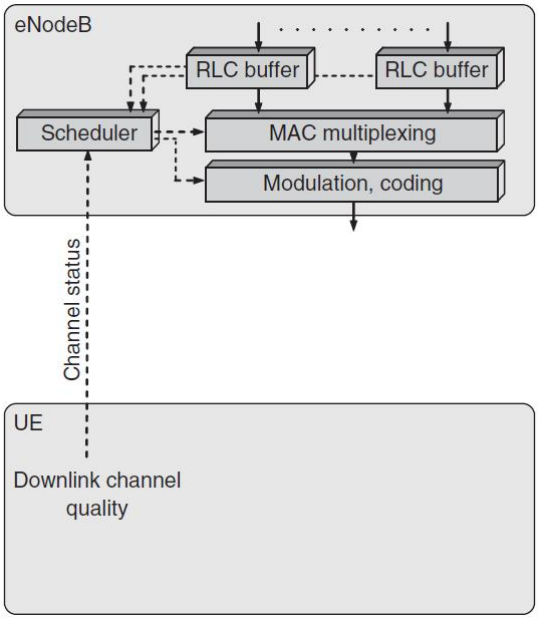

Figure 4.5: Downlink scheduling

The main idea of the scheduler, since it can exploit channel variations in time and frequency domain, is to schedule a transmission to a terminal with the best

channel conditions. Especially for low speed UEs where time domain channel variations not likely to change fast, the frequency domain channel variations can vary significantly, which gives LTE scheduler an advantage over earlier generation technologies like HSPA.

4.2.3 Discontinuous Reception (DRX)

To save UE battery DRX has two states configure *connected* and *idle* so that UE does not always have to monitor the downlink channels. The parameterization of DRX is a tradeoff between UEs battery life and latency e.g. for surfing the web and viewing a single webpage it is not beneficial to continuously receive information from the downlink channels, since the data showing the page has already been loaded on the device. On the other hand shorted idle period gives a faster response if new data has to be captured.

4.2.4 HARQ

HARQ provides robustness against transmission errors and as seen in Figure 4.3 it is a part of MAC layer functions but also a part of physical layer. There is only one HARQ entity at UE which handles number of parallel HARQ processes, where each process is associated with a HARQ identifier. HARQ is not applicable for all of the traffic; hence in downlink only for DL-SCH. HARQ function on MAC layer specifies which soft combining (Chase Combining (CC) or Incremental Redundancy (IR)) and which type of HARQ (independent, blanking or non-blanking) should be used. HARQ functionality on the physical layer is described in Chapter 4.3.3.

4.3 PHY Layer

The LTE physical layer is the lowest layer before sending the data from base station, also called enhanced NodeB (eNodeB) to UE. In downlink direction it is responsible for Cyclic Redundancy Check (CRC), coding, rate matching, modulation and mapping e.g. transport channels into physical channels as stated before. Figure 4.6 from [14] shows an overview of physical layer downlink transmission and its functions, which will be described in detail in the upcoming chapters.

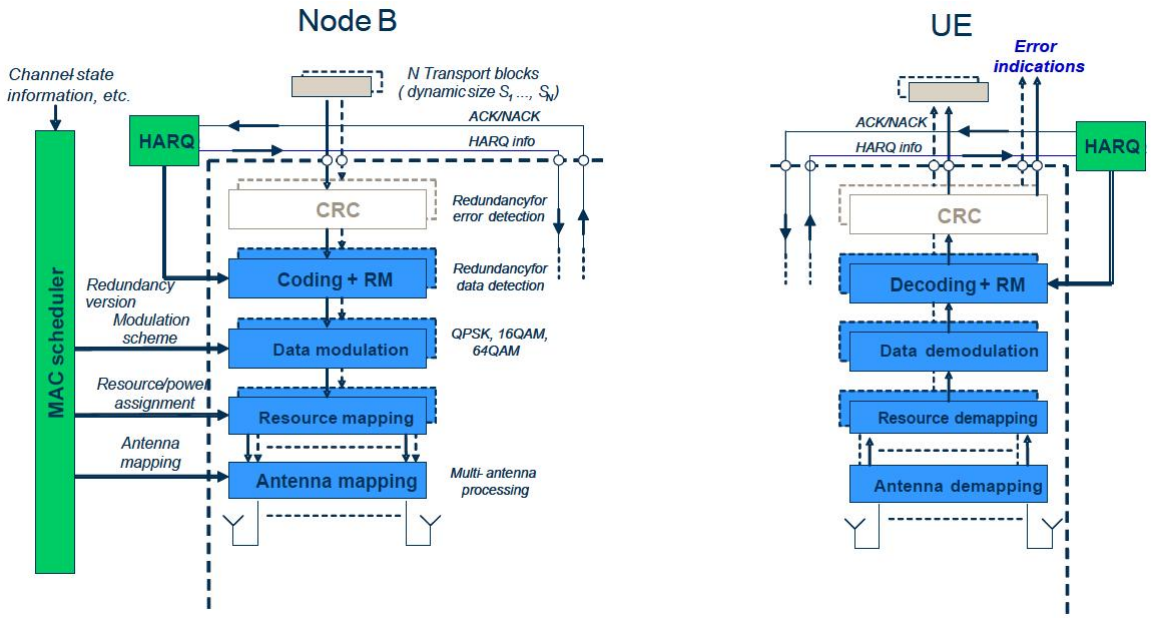

Figure 4.6: Physical layer function in downlink transmission

4.3.1 Channel coding

Channel coding is used to increase the reliability of the channel by adding redundancy to the information transmitted with the drawback of reducing the information rate.

4.3.1.1 CRC

In first step of physical layer downlink processing a 24 bit CRC is calculated for each data block for error detection at the receiver. If CRC detection fails at the receiver, e.g. HARQ will inform the transmitter about failed transmission and requests a retransmission according to which type of HARQ is used. If the input bits of a length A are listed as $a_0, a_1, \ldots, a_{A-1}$ and the parity bits of length L are denoted by $p_0, p_1, \ldots, p_{L-1}$. The parity bits are generated by using e.g. the following cyclic generator polynomial [10].

$$g_{CRC24B}(D) = \left[D^{24} + D^{23} + D^6 + D^5 + D + 1\right] \tag{4.1}$$

The encoding is performed in systematic form, where the polynomial

$$a_0 D^{A+23} + a_1 D^{A+22} + \ldots + a_{A-1} D^{24} + p_0 D^{23} + p_1 D^{22} + \ldots + p_{22} D^1 + p_{23} \quad (4.2)$$

is divided by corresponding 24 bit CRC polynomial and yields a remainder equal to 0:

$$a_0 D^{A+14} + a_1 D^{A+14} + \ldots + a_{A-1} D^{16} + p_0 D^{15} + p_1 D^{14} + \ldots + p_{14} D^1 + p_{15} \quad (4.3)$$

4.3.1.2 Turbo coding

Berrou, Glavieux and Thitimajasimha presented turbo codes and concept of iterative decoding to achieve near Shannon limit performance in 1996 [17]. It performs better than any other encoder at very low SNR. Turbo encoder consist two eight state convolutional encoders linked by an interleaver. LTE standard specifies a Parallel Concatenated Convolutional Code (PCCC) encoder with a coding rate of 1/3 and transfer function [10]:

$$G(D) = \left[1, \frac{g_1(D)}{g_0(D)}\right] \quad (4.4)$$

where

$g_0(D) = 1 + D^2 + D^3 = [1011]$

$g_1(D) = 1 + D + D^3 = [1101]$

Figure 4.7 illustrates the structure of 1/3 turbo encoder used in LTE. The output of the turbo encoder is given in equation (4.5).

$$d_k^{(0)} = x_k, \quad d_k^{(1)} = z_k, \quad d_k^{(2)} = z'_k \quad k = 0, 1, \ldots, K-1 \quad (4.5)$$

where

K is the number of input bits

x_k are called systematic bits

z_k are called first partity bits

z'_k are called second parity bits

The input bits respectively the output bits for the encoders interleaver are denoted $c_0, c_1, \ldots, c_{K-1}$ respectively $c_0, c_1, \ldots, c_{K-1}$ and the relationship is listed in equation (4.6) and (4.7).

$$c'_i = c_{\Pi(i)} \quad i = 0, 1, \ldots, K-1 \tag{4.6}$$

$$\Pi(i) = \left(f_1 i + f_2 i^2\right) mod K \tag{4.7}$$

The parameters f_1 and f_2 depend on the block size K and stated in the Table 5.1.3-3 in [10]. LTE turbo encoder has the maximum block size of 6144 bits, if this number is exceeded the code block is split into smaller ones and again new CRC is generated before going through the turbo encoder. For simplicity reasons the simulator was implemented with the maximum code block size of 6144 bits.

In LTE downlink direction adaptive modulation and coding schemes are used, which means different number of coded bits can change depending on the retransmission and channel conditions. With turbo codes, its performance is sensitive to the systematic bits; hence they should be transmitted in the first transmission attempt. To meet this requirements LTE uses so called circular buffer rate matching which is illustrated in Figure 4.8 from [46].

The from turbo encoder generated systematic bits (systematic) and two streams of parity bits (parity0 and parity1) are interleaved separately by so called sub block interleavers. The redundancy version (RV) starting from 0 sends as many systematic bits as possible. For retransmission, meaning further redundancy versions, the parity bits are alternately inserted into the message to increase the redundancy.

4.3.2 Modulation

As already stated in Chapter 3.4 depending on the channel conditions LTE can uses different modulation order starting from QPSK up to 64-QAM. This is done by the modulation mapper as written in LTE standard in Chapter 7 in [11]. Figure 4.9 from [22] shows a discrete OFDM system model.

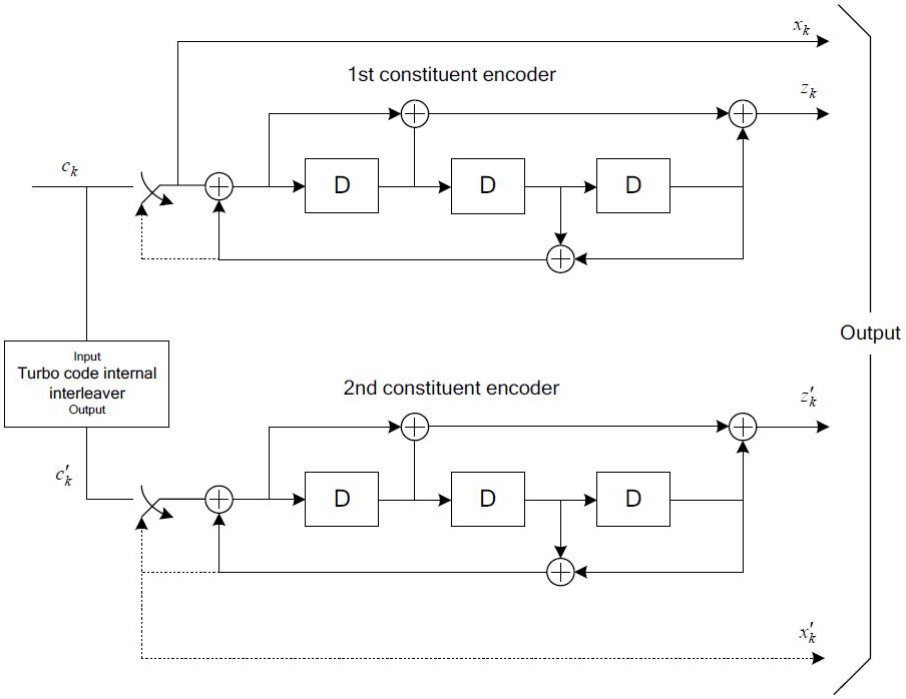

Figure 4.7: LTE turbo encoder structure

The data bits are grouped into block of N_c data symbols which can be written as a vector X. When performing IDFT or IFFT a cyclic prefix of length N_{cp} is inserted into X. The resulting signal can be mathematically described in equation (4.8).

$$s(n) = \begin{cases} \frac{1}{N_c} \sum_{k=0}^{N_c-1} X_k e^{j\frac{2\pi k(n-N_{cp})}{N_c}}. & n \in [0, N_c + N_{cp} - 1] \\ 0 & otherwise \end{cases} \tag{4.8}$$

4.3.3 HARQ

In LTE downlink asynchronous adaptive HARQ with soft combining is used see Chapter 3.7, therefore the erroneous packets are buffered at the receiver to combine it with the retransmission bits and to decode the message correctly. HARQ used in simulator for this thesis uses Chase combining method; where at each retransmission same message is sent and combined with the previous, not successfully decoded, message to increase the probability of correct transmission. An example of Chase combining was given in Figure 3.20.

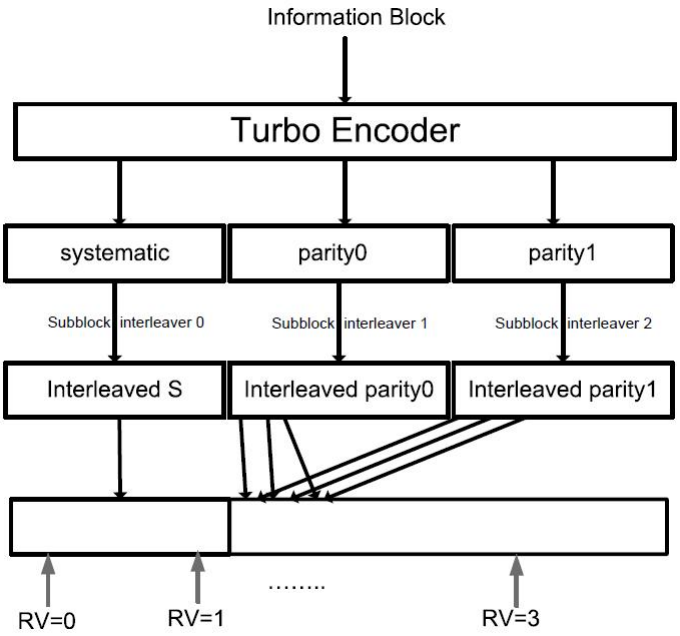

Figure 4.8: LTE rate matching for turbo codes

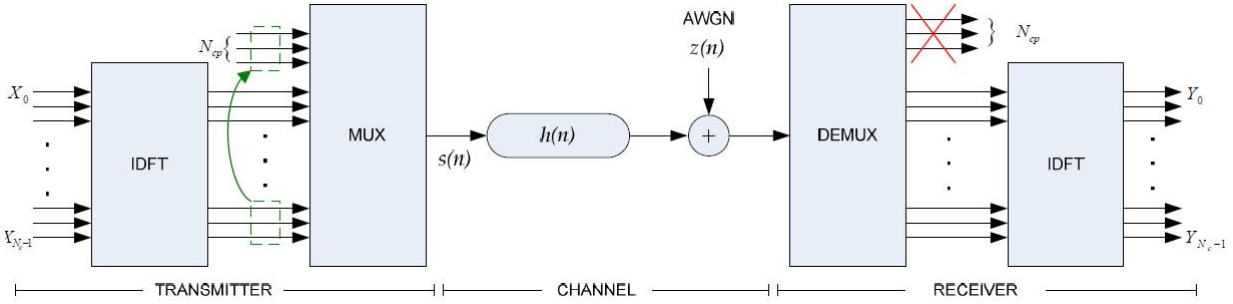

Figure 4.9: Discrete OFDM system model

Each HARQ process has three control information fields carried with the transmission [5]:

- *New data indicator (NDI)*: Is toggled when new data is delivered - 1 bit
- *RV*: Which redundancy version is used - 2 bits
- *Modulation and coding scheme (MCS)*: Which modulation and coding scheme is used - 3 bits

Chapter 5

Simulator

In next section of this chapter the simulation model from basic overview to more detailed functionality of the main elements in communication systems, transmitter, channel and receiver is introduced.

Furthermore different channel models used, e.g. Winner II, in the simulations are introduced and shown how they are implemented.

At the end the for thesis written simulator is verified to provide correct simulation results including correct modulation, HARQ functionality, transmit diversity, link adaptation and MIMO transmission.

5.1 System model

Figure 5.1 illustrates the model used in the simulator build for this thesis. As seen there is one transmitter (eNodeB) and one receiver (UE) and the UE is accepting data from eNodeB (downlink). In between there is a channel which can be selected from different International Telecommunication Union (ITU) channel models described in section 5.1.2.

Figure 5.2 shows the simulation flow, where at first simulation parameters are initialized including SNR, channel model, number of drops, number of frames etc.. First loop is made over initialized SNR values e.g. from 10 to 50 dB with 10 dB steps. Next loop is made over drops, meaning user is dropped in random place inside a cell and moved according to the set speed at the initialization process e.g. 3 km/h. The drop loop is followed by frame loop, where the number of sent frames is specified at the beginning of the simulation e.g. 100 frames. Then the typical sending and receiving process occurs, by sending data from transmitter

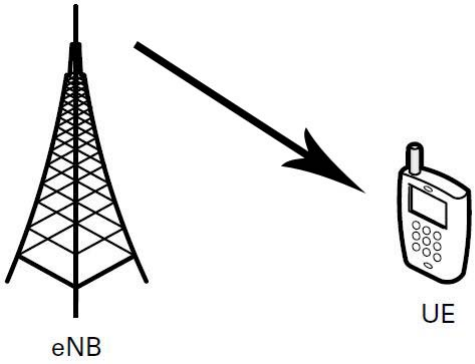

Figure 5.1: System model overview

over a certain channel conditions e.g. PedestrianA and received at UE. Before ending the frame loop statistics over the sent packets is collected for further use. After ending frame and drop loops the collected statistic data is summed up and values like Bit Error Rate (BER) and throughput are calculated, before starting the next SNR value loop. The simulation ends when SNR loop has run through all its values and the simulation results are saved for further use.

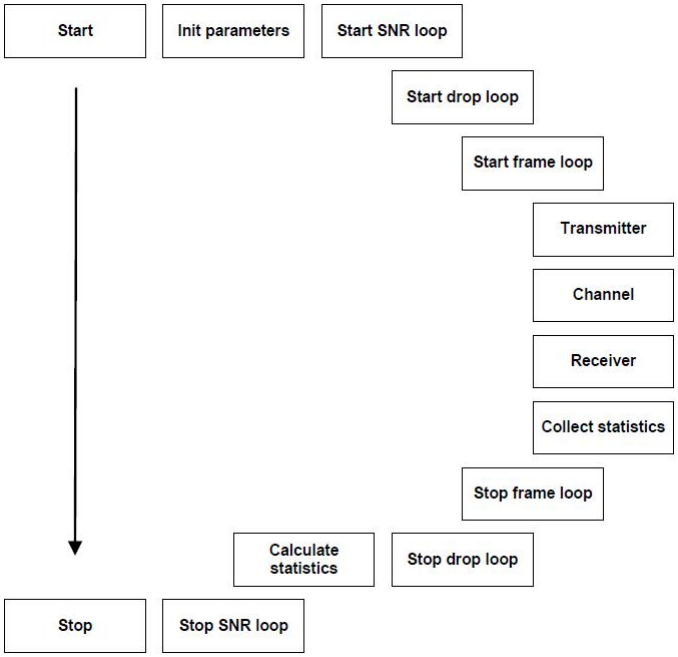

Figure 5.2: LTE Downlink simulation flow

5.1.1 Transmitter

Figure 5.3 shows the implemented 2x2 MIMO transmitter, where two random binary streams are mapped into different constellation diagrams and modulated with different subcarrier frequencies. Then as described for later channel estimation known pilot tones are inserted into the OFDM resource grid. Next signal spectrum length is increased by adding zeros and run through an IFFT block followed by cyclic prefix insertion as described in Chapter 3.3.3. Finally the transport blocks are mapped into the different antennas and sent to the receiver.

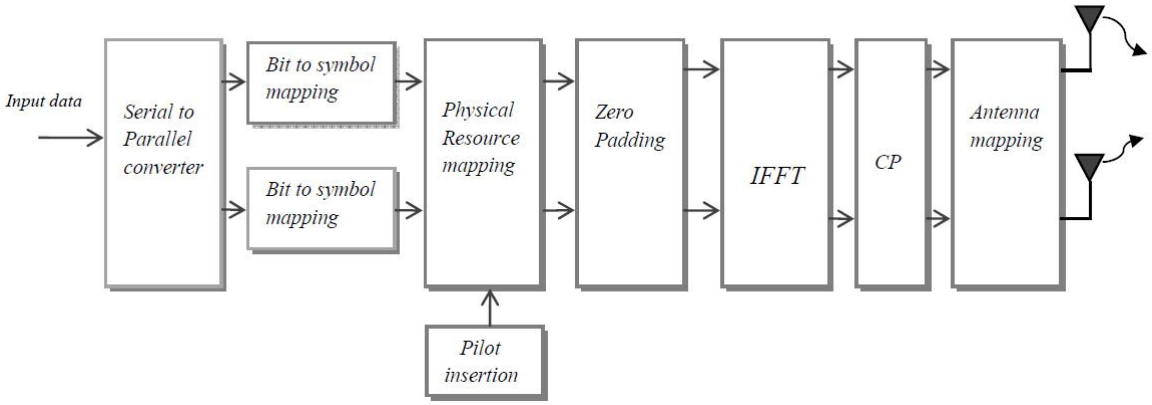

Figure 5.3: LTE Downlink 2x2 MIMO transmitter

5.1.2 Channel

The transmitted signal in real world results multipath propagation caused by following basic mechanisms:

- Line of sight propagation
- Specular reflections
- Diffraction caused by bending electromagnetic waves
- Diffusion or scattering
- Partial absorbtion e.g. transmission through objects

In the real world the number of paths is unknown, but for simulation purposes the number of paths is fixed enabling channel modeling. Good channel models are essential for analysis, design and development of telecommunication systems. The more realistic the model is the better the correlation between simulation and real world. There are many channel models to choose from. The next section discusses the ones used in the simulator.

The channel models are described as taps, where each taps corresponds to a certain delay and power. For the simulator the channel power values need to be normalized which is done in equation (5.1).

$$A_k = \sqrt{\frac{P_i}{\sum_{k=1}^{N} P_k}} \tag{5.1}$$

where

A_k is the channel tap normalized amplitude

P_i is the channel tap linear scale power

N is number of taps

5.1.2.1 Winner II model

For the final simulations, a special channel model with flat and short frequency response is used in order to see the differences between the simulation cases. The parameters for the Winner II channel model are taken from [42] and listed in Table 5.1. Winner II channel model is a suitable model for mobile indoor communication which adds some more actuality into this thesis.

5.1.2.2 Typical Urban model

Table 5.2 shows a six tap GSM typical urban channel, which in this thesis was used for MIMO 2x2 transmission verification [13].

Delay [ns]	Power [dB]
0	-15.2
5	-19.7
5	-15.1
5	-18.8
15	-16.3
15	-17.7
15	-17.1
20	-21.2l
25	-13.0
40	-14.6
80	-23.0
85	-25.1
110	-25.4
115	-24.8
150	-33.4
175	-29.6

Table 5.1: Winner II channel model parameters

Delay [μs]	Power [dB]
0	-3
0.2	0
0.5	-2
1.6	-6
2.3	-8
5.0	-10

Table 5.2: GSM 6 ray typical urban channel model parameters

5.1.3 Receiver

The receiver used in simulator has basically the same structure but opposite as in Figure 5.3 used transmitter. Instead of mapping demapping is used, cyclic prefix and padded zeros are removed and the received data is put through FFT block for demodulation.

It is to be noted, that at the receiver an MMSE channel estimator, as described in Chapter 3.4.3, is used to give feedback for the transmitter about the channel condition via Channel Quality Indicator (CQI) if higher modulation order can be

used to achieve better throughput.

5.1.4 Simulator verification

To ensure the informative value of the simulations, the used modules need to be verified by testing them separately before putting them together. In this section firstly the modulation and demodulation is tested to be working correctly by comparing the simulated Bit Error Rates (BER) with the BERs found in the literature before moving to HARQ verification, transmit diversity, link adaptation and MIMO transmission.

For modulation verification simple transmission scenarios are simulated and compared with known results from the theory e.g. one tap Rayleigh and Additive White Gaussian Noise (AWGN) channel are used to control the (BER) for given SNR values. These channel models are well known in the theory and the results can be easy compared to the theoretical values. Modulations used for BER verification are QPSK, 16-QAM and 64-QAM and the equations are taken from [27]. Table 5.3 shows parameter settings used for BER simulations.

First we define:

$$\gamma = \frac{E_b}{N_0} \tag{5.2}$$

$$Q(x) = \frac{1}{2} erfc\left(\frac{x}{\sqrt{2}}\right) = \frac{1}{\sqrt{\pi}} \int_{\frac{x}{\sqrt{2}}}^{\infty} e^{-t^2}\, dt \tag{5.3}$$

$$P(\gamma, L) = \frac{1}{2^L}\left(1 - \sqrt{\frac{\gamma}{1+\gamma}}\right)^L \sum_{k=0}^{L-1} \binom{L-1+k}{k} \frac{1}{2^k}\left(1 + \sqrt{\frac{\gamma}{1+\gamma}}\right)^k \tag{5.4}$$

where

E_b is energy over bit

N_0 is spectral noise density

$erfc(x)$ is complementary error function

L is number of branches

Parameter	Value
Bandwidth	5 MHz
Modulation	QPSK, 16-QAM or 64-QAM
Channel	AWGN or Rayleigh
Number of drops	50
Number of frames	100
FFT size	512
Number of subcarriers	300
Cyclic prefix	Normal
HARQ	No
Link adaptation	No
Pre-coding	No
Number of Tx antennas	1
Number of Rx antennas	1

Table 5.3: Basic simulation settings for BER simulation

5.1.4.1 BER QPSK

The bit error rate function for QPSK modulation for AWGN channel is shown in equation (5.5):

$$P_b = Q\left(\sqrt{2\gamma}\right) \tag{5.5}$$

and for Rayleigh channel:

$$P_b = P(\gamma, L) \tag{5.6}$$

The theoretical values and simulation results are compared in Figure 5.4.

5.1.4.2 BER 16-QAM

For Gray encoded 16-QAM modulation the bit error rate function for AWGN channel is:

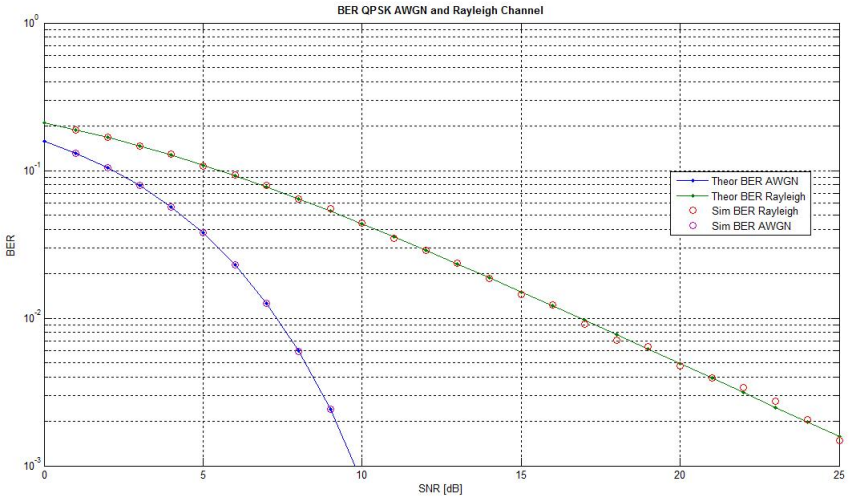

Figure 5.4: BER for QPSK modulation

$$P_b = \frac{3}{4}Q\left(\sqrt{\frac{4}{5}\gamma}\right) + \frac{1}{2}Q\left(3\sqrt{\frac{4}{5}\gamma}\right) - \frac{1}{4}Q\left(5\sqrt{\frac{4}{5}\gamma}\right) \tag{5.7}$$

and for Rayleigh channel:

$$P_b = \frac{3}{4}P\left(\frac{2}{5}\gamma, L\right) + \frac{1}{2}P\left(\frac{18}{5}\gamma, L\right) - \frac{1}{4}P\left(10\gamma, L\right) \tag{5.8}$$

The theoretical values and simulation results are compared in Figure 5.5.

5.1.4.3 BER 64-QAM

Again for Gray encoded 64-QAM modulated signal BER function for AWGN channel is described as:

$$P_b = \frac{7}{12}Q\left(\sqrt{\frac{2}{7}\gamma}\right) + \frac{6}{12}Q\left(\sqrt{\frac{18}{7}\gamma}\right) - \frac{1}{12}Q\left(\sqrt{\frac{50}{7}\gamma}\right) + \frac{1}{12}Q\left(\sqrt{\frac{162}{7}\gamma}\right) - \frac{1}{12}Q\left(\sqrt{\frac{338}{7}\gamma}\right) \tag{5.9}$$

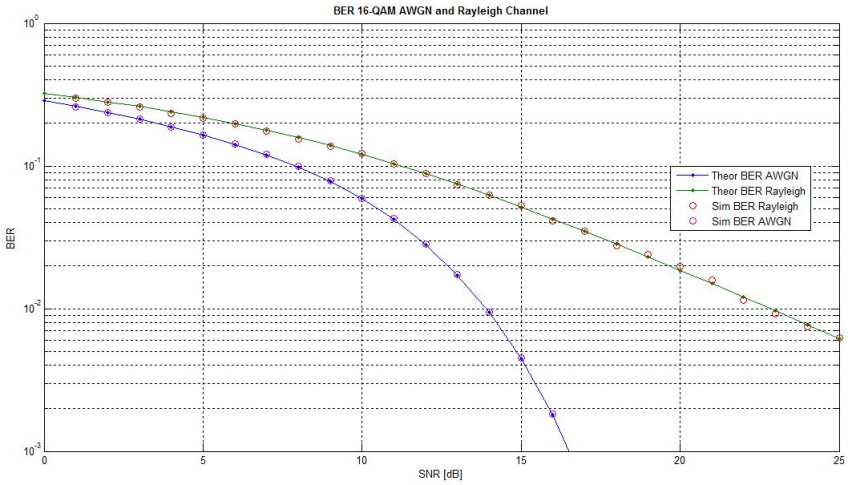

Figure 5.5: BER for 16-QAM modulation

and for Rayleigh channel:

$$P_b = \frac{7}{12}P\left(\frac{1}{7}\gamma, L\right)+\frac{6}{12}P\left(\frac{9}{7}\gamma, L\right)-\frac{1}{12}P\left(\frac{25}{7}\gamma, L\right)+\frac{1}{12}P\left(\frac{81}{7}\gamma, L\right)-\frac{1}{12}P\left(\frac{169}{7}\gamma, L\right) \tag{5.10}$$

The theoretical values and simulation results are compared in Figure 5.6.

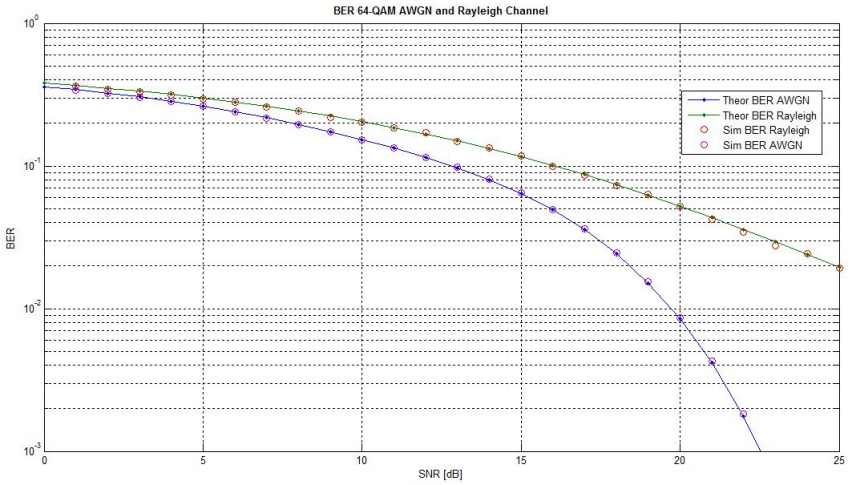

Figure 5.6: BER for 64-QAM modulation

The simulation results as shown in figures show good results where the simulated BER results are very close to the theoretical values. These tests confirm the modulation and demodulation working properly and the results received from the simulator are reliable. The small variation from theoretical results seen on Rayleigh channel BER curves can be explained by channels random number generator. To plan those it would need much more channel sent frames, but since the curves are very close to the theoretical values it is not considered as a needed procedure.

5.1.4.4 HARQ functionality

The HARQ functionality can be verified with various throughput simulations depending on SNR, where different throughput curves for different coding rates are simulated without HARQ functionality and then compared with the HARQ simulation throughput. The HARQ throughput should adapt to the best throughput curve for the given SNR.

To test the HARQ functionality QPSK modulation with different coding rates in AWGN channel was chosen and all other parameters used in simulation are the same as presented in Table 5.3. Table 5.4 from [12] shows according to which CQI index which modulation and coding rate is used in LTE standard.

Firstly, CQI indexes from one to six were simulated in an AWGN channel without HARQ retransmissions and throughput calculated and plotted as illustrated in

CQI Index	Modulation	code rate x 1024
0	out of range	
1	QPSK	78
2	QPSK	120
3	QPSK	193
4	QPSK	308
5	QPSK	449
6	QPSK	602
7	16-QAM	378
8	16-QAM	490
9	16-QAM	616
10	64-QAM	466
11	64-QAM	567
12	64-QAM	666
13	64-QAM	772
14	64-QAM	873
15	64-QAM	948

Table 5.4: CQI Index table

Figure 5.7.

Second the shannon capacity is calculated using the following equation:

$$C = FB \log_2 (1 + SNR) \tag{5.11}$$

where

C is system capacity (Shannon capacity)

B is bandwidth occupied by the data subcarriers

SNR is Sigal-to-Noise-Ratio

F is a correcting factor to cover some system losses

The bandwidh B is calculated according to [35]:

$$B = \frac{N_{sc} N_s N_{rb}}{T_{sub}} \tag{5.12}$$

where

N_{sc} is number of subcarriers in one resource block

N_s is number of OFDM symbols in one subframe

N_{rb} is number of resource blocks in selected system bandwidth

T_{sub} is the duration of one subframe

The correction factor F including CP and pilot sequence insertion losses [35]:

$$F = \frac{T_{frame} - T_{CP}}{T_{frame}} \frac{N_{sc} N_s/2 - 4}{N_{sc} N_s/2} \tag{5.13}$$

where

T_{frame} is frame duration

T_{CP} is total CP time of all OFDM symbols in one frame

For this HARQ simulation number of subcarriers was set to $N_{sc} = 11$, number of OFDM symbols $N_s = 14$, number of resource blocks $N_{rb} = 25$, length of a subframe $T_{sub} = 1$ ms, length of a frame $T_{frame} = 10 \cdot T_{sub} = 10$ ms and $T_{CP} = 20 \cdot 7 \cdot 4.7 \cdot 10^{-6}$s $= 658$ μs. The shannon capacity was plotted together with CQI indexes in Figure 5.7.

Next QPSK modulation with the highest coding rate was selected (CQI = 6) and HARQ functionality with Chase combining (CC) with maximum of three HARQ retransmissions was switched on and the simulation was run again and throughput plotted with the previous results. The number of drops and frames from Table 5.3 was changed to five respectively 1000 to minimize the number of lost statistic frames e.g. if 50th frame transmission is not successfull and the frame should be retransmitted with HARQ, it is lost because of reached number of maximum frames in that drop .The results are shown in Figure 5.8.

Figure 5.9 shows an example of HARQ where it is easier to calculate which code rate curves it will adapt to. The simulation is run under same conditions as the previous, AWGN channel with five drops and 1000 frames to be calculated; nevertheless the coding rate is changed. The coding rate is 2/3, which does not correspond to a CQI in the LTE standard as seen in Table 5.4, but it was implemented in the simulator to better see the different coding rates that HARQ

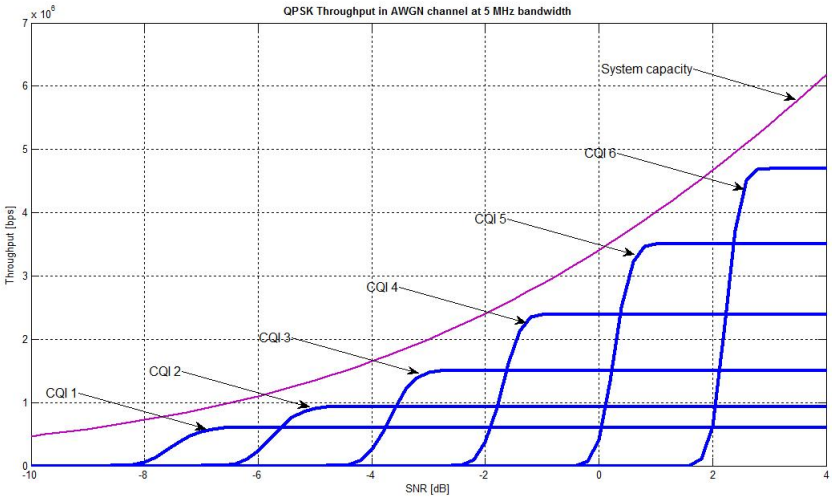

Figure 5.7: QPSK throughput for different coding rates

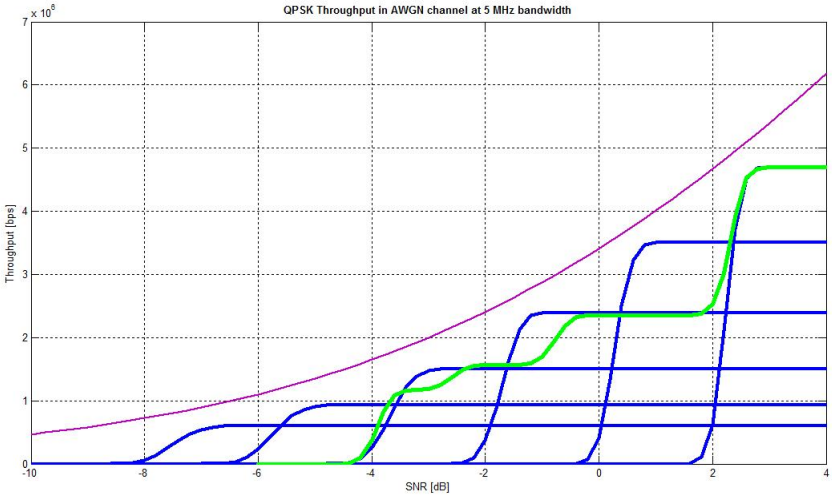

Figure 5.8: QPSK throughput with HARQ CC CQI = 6

	First Tx	1. reTx	2. reTx	3. reTx
Coding rate	$\frac{2}{3}$	$\frac{1}{3}$	$\frac{2}{9}$	$\frac{1}{6}$

Table 5.5: QPSK coding rates

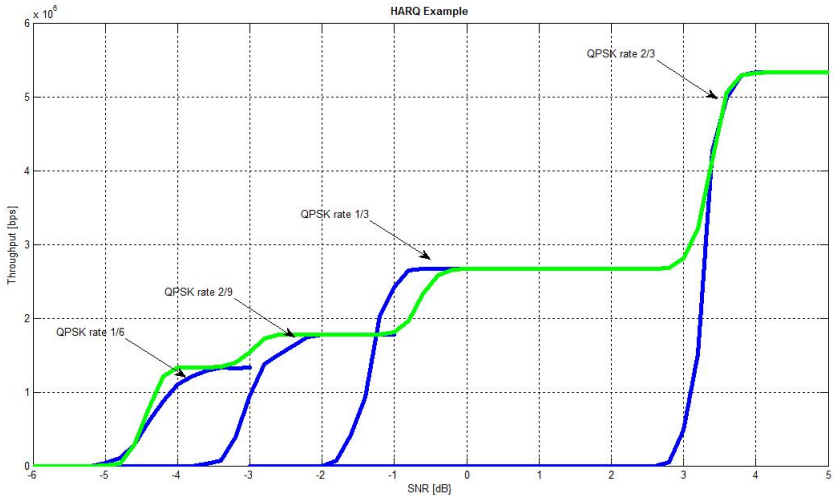

Figure 5.9: QPSK coding rate 2/3 throughput with HARQ IR

utilizes before reaching its maximum throughput. Table 5.5 shows the coding rates which are realized with QPSK rate 2/3 after each retransmission.

It is shown in the Figure 5.8 the benefit on HARQ, without HARQ for CQI = 6 the throughput is larger than zero around SNR = 2 dB, but with retransmissions data can already be correctly encoded at SNR = -5.5 dB. As stated at the beginning of the section, the throughput curve adapts to the best fitting CQI curve as far the coding rates are matching. One can see around SNR = -3 and -1 dB, the curve is not achieving its maximum throughput value. This effect is caused by Chase combining used for retransmission, where not only data, but redundancy bits are resent. This phenomenon is called SNR loss. As a result HARQ implementation can be considered as working properly.

5.1.4.5 Transmit diversity

For transmit diversity testing two transmission antennas with QPSK modulation (CQI = 5) were added into simulation, where Rayleigh one tap channel was used and BER curve calculated. Transmit diversity should result to so called SNR gain, where the BER curve is moved to the left, meaning better BER rate is achieved at the receiver side. Figure 5.10 shows the simulation result compared with single antenna QPSK modulation over Rayleigh one tap channel.

One can see from Figure 5.10 the SNR gain provided by transmit diversity, the BER curve is shifted to the left giving better BER for given SNR. Therefore

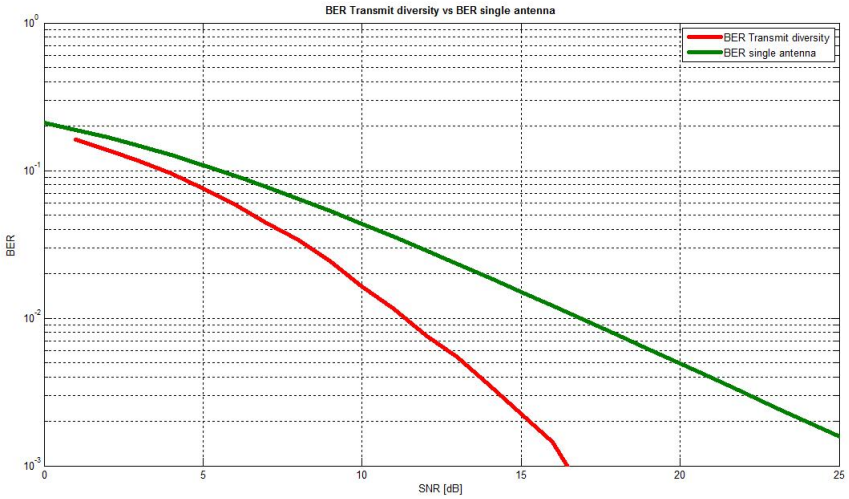

Figure 5.10: QPSK Trasmit diversity vs QPSK single antenna Rayleigh channel

transmit diversity can be assumed as working properly.

5.1.4.6 Link adaptation

Link adaptation was tested at system bandwidth set to 5 MHz without channel estimation (no pilot tones used). As a reference Figure 5.7 was used, where throughput curves with different coding rates using QPSK modulation (CQI = 1 to CQI = 6) were plotted. Using link adaptation should pick the best CQI matching the current SNR value and as an outcome one should get a curve fitting the best coding rate and throughput for given SNR e.g for SNR = 1 dB link adaptation must pick CQI = 5. Figure 5.11 shows the simulation results.

Figure 5.11 shows how link adaptation chooses the correct coding rate for the given SNR and adapts to the best possible throughput curve. Therefore the result confirms link adaptation working correctly and can be assumed as implemented in proper way.

5.1.4.7 MIMO transmission

For MIMO transmission verification a reference article [1] Table 2 was used to compare their throughput results with the simulator. The simulation was made for three different modulation QPSK, 16-QAM and 64-QAM with different coding rates and the maximum throughput was compared with the results from the

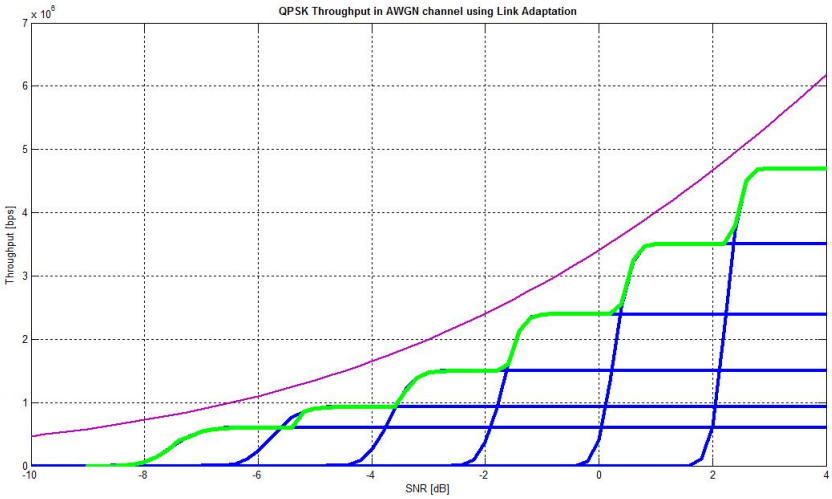

Figure 5.11: Link adaptation test with no channel estimation

reference. The calculation were made in AWGN channel with system bandwidh of 20 MHz and number of resource block was set to $N_{rb} = 100$. The results are listed in Table 5.6 as throughput in Mbps and spectral efficiency in bit/Hz/s.

	Simulator		Reference	
	[Mbps]	**[bit/Hz/s]**	**[Mbps]**	**[bit/Hz/s]**
QPSK 1/2	30.4	2.00	31.1	1.99
QPSK 3/4	45.6	3.00	46.9	3.01
QPSK 4/5	48.7	3.20	50.1	3.21
16-QAM 1/2	60.8	4.00	62.6	4.01
16-QAM 2/3	81.1	5.34	83.4	5.35
16-QAM 3/4	91.2	6.00	93.8	6.01
64-QAM 2/3	121.6	8.00	125.1	8.02
64-QAM 3/4	136.8	9.00	140.8	9.03
64-QAM 4/5	145.9	9.60	150.2	9.63

Table 5.6: MIMO 2x2 Throughput verfication

The simulation results are close to the reference. The difference between the throughputs can be explained by the subcarrier usage in shared channel and bandwidth allocation in both systems. Equation (5.14) shows how the throughput can be calculated from modulation order, coding rate and subcarrier usage in shared channel.

$$T_r = N_{bits} R N_{sub} \tag{5.14}$$

where

T_r is throughput

N_{bits} is number of bits per symbol

R is code rate

N_{sub} is number of subcarriers per second

As an example for subcarrier usage, calculation 64-QAM with coding rate 4/5 is taken from Table 5.6. For 145.9 Mbps $N_{sub} \approx 30400$ subcarriers/ms for both streams, divided by two because of MIMO transmission one gets 15200 subcarriers/ms for one stream for 20 MHz system bandwidth. Same calculation for the values taken from [1] the number of subcarriers for one stream is approximately 15600 subcarriers/ms.

The MIMO system theoretical capacity is calculated using equation (5.11), but the logarithm term is replaced by the term shown in equation (5.15) which is also called spectrum density.

$$E = \log_2 \left(\det \left[I_{n_R} + \frac{SNR}{n_T} H^H H \right] \right) \tag{5.15}$$

where

E is spectral efficiency

I is identity matrix

n_T is number of transmitter antennas

n_R is number of receiver antennas

SNR is Sigal-to-Noise-Ratio

H^H is Hermite conjugate of n_T x n_R channel matrix

The channel matrix elements $\{h_{ij}\}$ are constructed from two normal independent and normal distributed variables α and β, which makes $|h_{ij}|$ Rayleigh distributed Rayleigh distributed random value [27].

$$h_{ij} = \alpha + j\beta \tag{5.16}$$

In Figure 5.12 same simulation conditions were used as in [1], meaning six ray typical urban channel and 20 MHz system bandwidth. The throughput was divided by the number of subcarriers per ms to get comparable results with the equation (5.15) in the same figure.

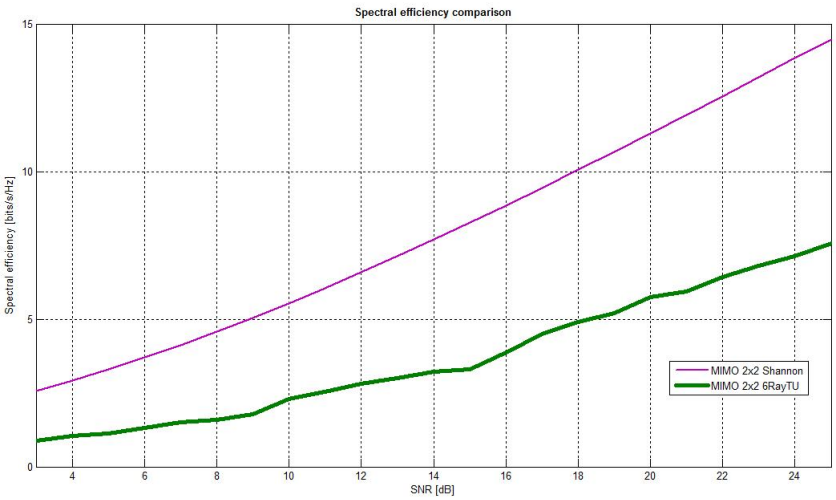

Figure 5.12: MIMO 2x2 spectral efficiency comparison

Comparing the spectral efficiency curves with the calculated 2x2 MIMO Shannon efficiency, it is seen that there is huge ca. 10 dB difference between the simulated and the theoretical values. Few reasons for not achieving the theoretical maximum throughput are the use of realistic modulation and coding and MMSE receiver, which is known not to be ideal. Moreover CRC insertion as illustrated in Chapter 4.3.1.1 is also affecting the throughput, as well as CP addition and usage of pilot tones. Therefore the results including Shannon spectral efficiency calculation can be considered as correct and MIMO 2x2 transmission assumed working properly. The comparison of the simulated spectral efficiency outcome with the references [1] and [37], show similar result.

Chapter 6

Multicodeword-MIMO Performance

This chapter describes the simulation parameters used to investigate HARQ throughputs including Winner II indoor channel model. The results are listed separately and compared in the final part of this chapter.

The three simulation cases are run under same circumstances and only the HARQ functionality is changed. Table 6.1 lists parameters used in all three simulations. Preliminary tests have shown to run the simulation from SNR range -12 dB to 25 dB incrementing 1 dB at each step. The Winner II channel parameters are listed in Table 5.1. The modulation rates depends on the channel conditions reported as CQI by link adaptation described in Chapter 3.5. The BLER for the first transmission is set to 10 % as seen in Figure 3.13

For the final simulation the number of drops was raised to 1000 to achieve high amount of channel condition samples. The simulation of one point takes around 12 hours to complete. To save time the number of frames was dropped to 20 and 10 are collected for the statistics. The first 10 frames are ignored, since the simulator has not reached its steady state.

6.1 Simulation Results

In Figure 6.1 all the throughput curves and the system capacity are plotted in the same graph. The thoughts made before simulation are approved showing the independent HARQ processes being the most effective method in terms of throughput and non-blanking method being the worst of the three cases. As seen from the plot, the independent HARQ and blanking method are very close to each other.

Parameter	**Value**
Bandwidth	10 MHz
Modulation	QPSK, 16-QAM or 64-QAM
Channel	Winner II
Channel estimation	Ideal
Receiver	MMSE
Number of drops	1000
Number of frames	20
SNR range	-12 to 25 dB with 1 dB steps
FFT size	1024
Number of subcarriers	600
Subcarrier symbols	7600 1/ms
First Tx BLER	10 %
Cyclic prefix	Normal
HARQ	Yes
Link adaptation	Yes
Pre-coding	No
Number of Tx antennas	2
Number of Rx antennas	2

Table 6.1: HARQ simulation parameters

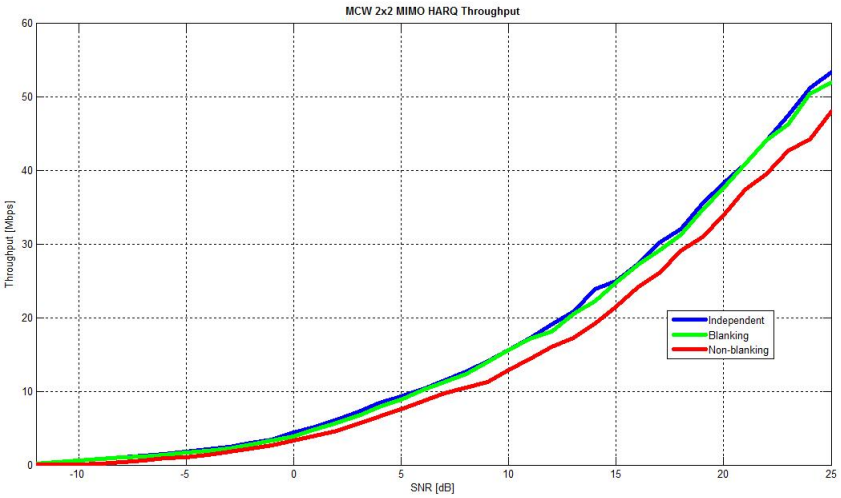

Figure 6.1: Multicodeword-MIMO HARQ performance

One might ask why is the throughput curve not showing any envelope behavior as seen in Figure 5.11 where single codeword SISO link adaptation was tested. Due the link adaptation for MCW MIMO different antennas can have different modulation and coding index for the given SNR depending on the current channel conditions. The envelope disappears since the average throughput from different CQI indexes is taken.

As it comes to Shannon capacity as seen in Figure 5.12, there is still lot capacity left to make a better MIMO transmission in terms of throughput. In other words the MIMO spectral efficiency can still be improved for further standards. There are of course some losses caused by non ideal transceivers, pilots tones, CRC insertion and realistic modulation, although there is still lot to investigate on MIMO transmissions.

6.2 Comparison

To better see the difference between the HARQ cases, the throughput ratio is calculated using the best, independent HARQ, as reference. The results are seen in Figure 6.2.

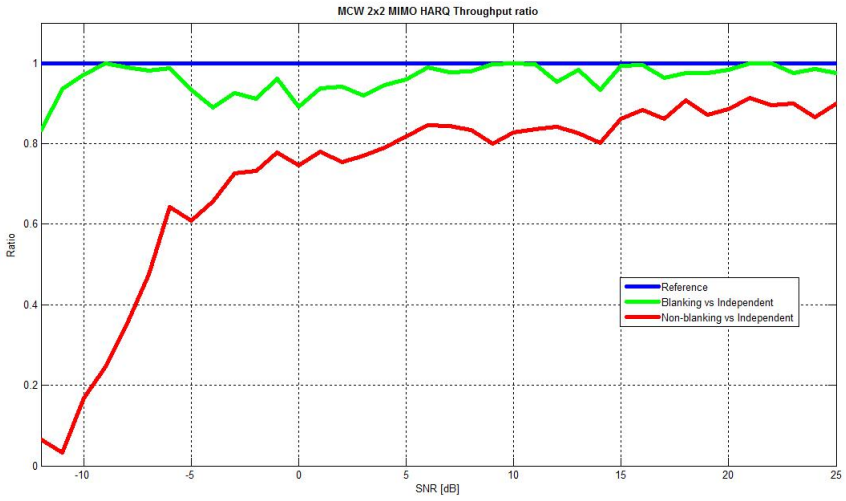

Figure 6.2: MCW MIMO HARQ Throughput ratio

The plot shows for non-blanking HARQ transmission a trend for growing SNR values the ratio gets better. The non-blanking method works poorly at low SNR as seen between -12 and -4 dB. At SNR = 5 dB the ratio is always over 80 %.

This method is clrearly the worst, but for growing SNR the throughput gets significantly better than for lower values.

Blanking HARQ method shows more or less constant ratio over 90 %. This method is very close to the best transmission method. From SNR = 5 dB the ratio hardly drops under 95 %.

Both of the last figures confirm that independent HARQ is the best, non-blanking one is the worst and blanking is in between. The blanking HARQ method is very close to the independent HARQ where it can achieve at good SNR ratio up to 98-99 % from the original values.

Chapter 7

Conclusion

In this thesis three different HARQ techniques have been investigated. To sum up the simulation results, HARQ method with two independent HARQ processes is the best method in terms of throughput, nevertheless blanking technique comes very close to it.

The difference between these three techniques is how the retransmissions are handled. In independent HARQ every codeword has its own ACK/NACK, where in blanking and non-blanking there is only one ACK/NACK for two codewords. Therefore in blanking it is known which codeword was decoded correctly. As one can see in Figure 6.2, this makes a huge, up to 20 %, difference between those methods. In non-blanking lot of resources are wasted. If one codeword is decoded correctly and the other is not the correctly received codeword is ignored and resent again.

The fact that the simulation results are quite far away from the theoretical maximum has to be accepted. When comparing simulation results with the references stated in previous chapters, the numerical results are correct as well as the formula to calculate the Shannon spectral efficiency.

One question remains, why even bother to compare different HARQ methods, when it already a priori known which method is the best. For sure, the method with two independent HARQ processes for two codewords is the best, but also most difficult to implement. Hence, it is better to look for alternatives, which are easier to implement in software and hardware and may work near as good as the more complex one. Therefore, there are many other factors than just the best throughput, complexity, implementation and costs are aspects which need also to be taken into account while designing new standards.

To sum up the knowledge gained from this work, as the topic becomes relevant for

the upcoming LTE-Advanced standard. It was shown that non-blanking HARQ method is a good candidate for the HARQ process bundling in uplink as discussed in [25].

7.1 Future work

The simulator made for this thesis can imitate a single user MIMO downlink transmission in one cell, so there is lot of room for expansion. Before adding more parts into it, my personal suggestion is to optimize the current code. The code has bottlenecks e.g. CQI reporting is very slow, since the BLER has to be calculated and examined. There are few ways to optimize the speed e.g. compiling some function into c-code, which is already done for the turbo encoder. Other ways to make the code run faster is vectorizing different for loops to run the code significantly smoother. Speed optimization is very welcome, since for the last test simulations one SNR point took more than 12 hours to simulate on 2.1 GHz duo processor with 4 GB of memory.

Next suggestion for the future work will be designing a Graphical User Interface (GUI) into the current simulator. Since the communication institute would like to have a tool to demonstrate during lectures or seminars, it is easier to have a simple interface with parameters to choose, than searching for them in the source code. This simulator has many parameters, which may confuse people not so familiar with it.

Moreover, expansion of the current simulator e.g. into multiple users or multiple cell would be an interesting work to do. Since the simulator is measuring only downlink traffic, next task could be adding uplink direction into it. This may be an attractive part to examine cell traffic from base station point of view, which can awake interest of mobile operators. Lastly, the investigation of the causes, why multi antenna transmission efficiency is so far away from the theoretically achievable maximum. What are the causes for the losses and how can the transmission be even more optimized.

References

[1] 3GPP. Throughput Evaluations Using MIMO Multiplexing in Evolved UTRA Downlink, June 2005. R1-050664.

[2] 3GPP. Views on OFDM Parameter Set for Evolved UTRA Downlink, May 2005. TSG RAN WG1 Meeting #41, Athens, Greece.

[3] 3GPP. Implications of MCW MIMO on DL HARQ, February 2006. R1-060459.

[4] 3GPP. Physical layer apsects for evolved Universal Terrestial Radio Access, October 2006. TR 25.814 v7.1.0.

[5] 3GPP. Consideration on control signalling for MIMO-HARQ in E-UTRA downlink, March 2007. R1-071556.

[6] 3GPP. Overview of 3GPP Release 8: Summary fo all Release 8 Features, November 2008. Release 8 v0.0.3.

[7] 3GPP. Physical Channels and Modulation, May 2009. TR 36.211 v8.7.0.

[8] 3GPP. 3GPP Technical releases, July 2010. http://www.3gpp.org/releases.

[9] 3GPP. Medium Access Control (MAC) protocol specification, March 2010. TR 36.321 v9.2.0.

[10] 3GPP. Multiplexing and channel coding, March 2010. TS 36.212 v9.1.0.

[11] 3GPP. Physical Channels and Modulation, March 2010. TS 36.211.

[12] 3GPP. Physical layer procedures, March 2010. TS 36.213.

[13] 3GPP. Radio Access Network; Radio transmission and reception, September 2010. TS 45.005.

[14] 3GPP. Services provided by the physical layer, March 2010. `TS 36.302 v9.1.0`.

[15] Muhammad Saad Akram. Pilot-based Channel Estimation in OFDM systems, August 2007. Master Thesis.

[16] S. M. Alamounti. A Simple Transmit Diversity Technique for Wireless Communication. *IEEE Journal Select. Areas Communications*, 16(8):1451–1458, 1998.

[17] Claude Berrou and Alain Glavieux. Near Optimum Error Correcting Coding And Decoding: Turbo-Codes. *IEEE Transactions on Communications*, 44(10):1261–1271, 1996.

[18] Ernst Bonek. The MIMO Radio Channel, September 2006. `Presentation, Technische Universtät, Wien, Austria`.

[19] David Chase. Code combining - A Maximum-Likelihood Decoding Approach for Combining an Arbitrary Number of Noisy Packets. *IEEE Transactions on Communications*, 33(5):385–393, 1985.

[20] Jung-Fu Cheng. Coding Performance of Hybrid ARQ Schemes. *IEEE Transactions on Communications*, 54(6):1017–1029, 2006.

[21] Erik Dahlman, Stefan Parkvall, Johan Sköld, and Per Beming. *HSPA and LTE for Mobile Broadband.* Academic Press, Oxford, United Kingdom, 2008.

[22] Marc Engels. *Wireless OFDM Systems, How to make them work?* Kluwer Academic Publishers, Massachusetts, USA, 2002.

[23] Ericsson. LTE - an introduction, June 2009. Whiteparer avaiable at `http://www.ericsson.com/res/docs/whitepapers/lte_overview.pdf`.

[24] Pål Frenger, Stefan Parkvall, and Erik Dahlman. Performance Comparison of HARQ with Chase Combining and Incremental Redundancy for HSDPA. *Proceedings of the IEEE Vehicular Technology Conference (VTC 2001 Fall)*, 3:1829–1833, 2001.

[25] et al. Gilberto Berardinelli. Link parameters bundling across multiple Component Carriers in LTE-A Uplink, February 2010. `Department of Electronic Systems, Aalborg University, Denmark`.

[26] A. J. Goldsmith and P. P. Varayia. Capacity of Fading Channels with Channel Side Information. *IEEE Transactions on Information Theory*, 43(6):1986–1992, 1997.

[27] Andrea Goldsmith. *Wireless Communications*. Cambridge University Press, New York, USA, 2005.

[28] Seong Taek Chung Goldsmith and A. J. Goldsmith. Degrees of Freedom in Adaptive Modulation: A Unified View. *IEEE Transactions on Communications*, 39(9):1561–1571, 2001.

[29] Jessica Heyman. Intercell Interference Management in and OFDM-based downlink, June 2006. Master Thesis.

[30] Harri Holma and Antti Toskala. *LTE for UMTS*. John Wiley & Sons Ltd., West Sussex, United Kingdom, 2009.

[31] Mohamed Ibnkahla. *Signal Processing for Mobile Communications - Hand book*. CRC Press, Florida, USA, 2005.

[32] Mohinder Jankiraman. *Space-Time Codes and MIMO Systems*. Artech House Boston, London, United Kingdom, 2004.

[33] Farooq Khan. *LTE for 4G Mobile Broadband*. Cambridge University Press, Cambridge, United Kingdom, 2009.

[34] M. E. O. Lierida. Adaptive Radio Resource Management for VoIP and Data Traffic in 3GPP LTE Networks, March 2008. Master Thesis.

[35] Chirstian Mehlführer, Marting Wrulich, Josep Colom Ikuno, Dagman Bosanska, and Markus Rupp. Simulating the Long Term Evolution physical layer. August 2009.

[36] Asad Mehmood and Waqas Aslam Cheema. Channel estimation for LTE downlink, September 2009. Master Thesis.

[37] Preben Mogensen, Wei Na, István Z. Kovács, Frank Frederiksen, Akhilesh Pokhariyal, Klaus I. Pedersen, Troels Kolding, Klaus Hugl, and Markku Kuusela. LTE Capacity compared to the Shannon Bound. April 2007.

[38] Hyung Myung, Junsung Lim, and David Goodman. Single Carrier FDMA for Uplink Wireless Transmission. *IEEE Vehicular Technology Magazine*, 1(3):30–38, 2006.

[39] Ammar Osman. Low-complexity OFDM transveiver design for UMTS-LTE, January 2007. Master Thesis.

[40] Claude Östges and Bruno Clerckx. *MIMO Wireless Communications: From Realworld Propagation to Space-Time Code Design*. Elsevier, London, United Kingdom, 2007.

[41] Jim Pearce. What's all this $\frac{E_b}{N_0}$ Stuff, Anyway?, Fall 2000. `Article from Spread Spectrum Scene Online at: http://http://www.sss-mag.com/ebn0.html`.

[42] et al. Pekka Kyösti. WINNER II Channel Models, February 2008. `IST-4-027756 WINNER II D1.1.2 V1.2`.

[43] Abraham Peled and Antonio Ruiz. Frequency Domain Data Transmission using Reduced Computational Complexity algorithms. *Proceedings of the IEEE International Conference on Acoustics, Speech and Signal Processing*, 5:964–967, 1980.

[44] Michael Pursley and Stuart Sandberg. Incremental-Redundancy Transmission for Meteor-Burst Communications. *IEEE Transactions on Communications*, 39(5):689–702, 1991.

[45] Sanjay Kumar Sarkar. A Long Term Evolution (LTE) Downlink DL inspired channel simulator using the SUI 3 channel model, August 2009. Master Thesis.

[46] Stefania Sesia, Matthew Baker, and Issam Toufik. *LTE - the UMTS Long Term Evolution: From Theory to Practice*. John Wiley & Sons Ltd., West Sussex, United Kingdom, 2009.

[47] Jan-Jaap van Beek, Ove Edfors, Magnus Sandell, Sarak Kate Wilson, and Per Ola Börjesson. On Cannel Estimation in OFDM Systems. *Proceedings of the IEEE Vehicular Technology Conference (VTC'95)*, 2:815–819, 1995.

[48] Jim Wight. The OFDM Challenge, November 2008. `http://www.commsdesign.com/story/OEG20011023S0040`.

[49] Jim Zyren and Dr. Wes McCoy. Overview of the 3GPP Long Term Evolution Physical Layer, July 2007. `White paper 3GPPEVOLUTIONWP`.